

# Comparison of artificial neural networks and reservoir models for simulating karst spring discharge on five test sites in the Alpine and Mediterranean regions

Guillaume Cinkus<sup>1</sup>, Andreas Wunsch<sup>2</sup>, Naomi Mazzilli<sup>3</sup>, Tanja Liesch<sup>2</sup>, Zhao Chen<sup>4</sup>, Nataša Ravbar<sup>5</sup>,  
5 Joanna Doummar<sup>6</sup>, Jaime Fernández-Ortega<sup>7</sup>, Juan Antonio Barberá<sup>7</sup>, Bartolomé Andreo<sup>7</sup>, Nico  
Goldscheider<sup>2</sup> and Hervé Jourde<sup>1</sup>

<sup>1</sup>HydroSciences Montpellier (HSM), Univ. Montpellier, CNRS, IRD, 34090 Montpellier, France

10 <sup>2</sup>Karlsruhe Institute of Technology (KIT), Institute of Applied Geosciences, Kaiserstr. 12, 76131 Karlsruhe, Germany

<sup>3</sup>UMR 1114 EMMAH (AU-INRAE), Université d'Avignon, 84000 Avignon, France

<sup>4</sup>Institute of Groundwater Management, Technical University of Dresden, 01062 Dresden, Germany

<sup>5</sup>ZRC SAZU, Karst Research Institute, Titov trg 2, 6230 Postojna, Slovenia

<sup>6</sup>Department of Geology, American University of Beirut, PO Box 11 - 0236/26, Beirut, Lebanon

15 <sup>7</sup>Department of Geology and Centre of Hydrogeology, University of Málaga (CEHIUMA), 29071 Málaga, Spain

*Correspondence to:* Guillaume Cinkus (guillaume.cinkus@umontpellier.fr)

**Abstract.** Hydrological models are widely used to characterise, understand and manage hydrosystems. ~~Data-driven~~Lumped parameter models are of particular interest in karst environments given the complexity and heterogeneity of these systems. There is a multitude of ~~data-driven~~lumped parameter modelling approaches, which can make it difficult for a manager or  
20 researcher to choose. We therefore conducted a comparison of two ~~data-driven~~lumped parameter modelling approaches: artificial neural networks (ANN) and reservoir models. We investigate five karst systems in the Mediterranean and Alpine regions with different characteristics in terms of climatic conditions, hydrogeological properties and data availability. We compare the results of ANN and reservoir modelling approaches using several performance criteria over different hydrological periods. The results show that both ANN and reservoir models can accurately simulate karst spring discharge,  
25 but also that they have different advantages and drawbacks: (i) ANN models are very flexible regarding the format and amount of input data, (ii) reservoir models can provide good results even with ~~short~~few years of relevant discharge in the calibration periods, and (iii) ANN models seem robust for reproducing high-flow conditions while reservoir models are superior for reproducing low-flow conditions. However, both modelling approaches struggle to reproduce extreme events (droughts, floods), which is a known problem in hydrological modelling. For research purposes, ANN models have shown to  
30 be useful to identify recharge areas and delineate catchment, based on insights into the input data. Reservoir models are adapted to understand the hydrological functioning of a system, by studying model structure and parameters.

## 1 Introduction

Karst systems are complex and heterogeneous media. High contrasts in porosity and permeability induce a high variability in infiltration and internal flow processes (Bakalowicz, 2005; Ford and Williams, 2007) which can be difficult to assess.

35 Considering the increasing demand for water and that around 9 % of the world's population (up to 90 % in some parts of the Mediterranean area) depends on karst water resources for drinking water supply (Stevanović, 2019), the characterisation of karst systems functioning and water availability become a major challenge for water resource management. Among the numerous methods to study karst systems (Goldscheider, 2015), hydrological models are useful to characterise karst functioning, and specially to predict the impact of climate and land use changes (Hartmann et al., 2014). Hydrological

40 models can be grouped into ~~data-driven~~lumped parameter and distributed approaches (Kovács and Sauter, 2007). While distributed models divide a karst system into a two- or three-dimensional grid, for which each cell is assigned appropriate hydraulic parameters and system states, ~~data-driven~~lumped parameter models are based on the mathematical analysis of input data (e.g. precipitation, temperature) for simulating spring discharge time series. They include (i) "black-box" models such as neural networks-based approaches, which use no a priori information about the functioning of a system; and (ii)

45 ~~reservoir~~"conceptual" models, which are based on a conceptual representation of a karst system – e.g., for the reservoir models, a succession of one or several reservoirs using simplified physical transfer functions.

The choice of a modelling approach depends mainly on the objective of the study, but also on the current knowledge of the system, ~~and~~ the available data, and regional/institutional preferences (Addor and Melsen, 2019). For karst systems, the available data are often scarce and poorly reflect the heterogeneity of the meteorological and karst processes. Distributed

50 models require a lot of diverse data with high spatial and temporal resolution for defining physical parameters and thus can be tough to use in a scarce data context (Hartmann et al., 2014). On the other hand, ~~data-driven~~lumped parameter models permit studying complex and heterogeneous karst systems without requiring extensive meteorological and system-related data with high spatial resolution. ~~Both "black box" and reservoirs models are therefore relevant for operational and research applications.~~ Artificial neural networks (ANN) have been successfully used to simulate karst spring discharge (Kurtulus and

55 Razack, 2007; Hu et al., 2008; Meng et al., 2015; Wunsch et al., 2022), predict and forecast water flood/inrush (Wu et al., 2008; Kong A Siou et al., 2011) and manage the exploitation of karst aquifers (Yin et al., 2011; Kong A Siou et al., 2015). Reservoir models also have been successfully used to simulate karst spring discharge (Fleury et al., 2007; Dubois et al., 2020), manage the exploitation of karst aquifers (Fleury et al., 2009; Zhou et al., 2021), as well as characterise specific functioning in karst systems (~~Tritz et al., 2011~~; Perrin et al., 2003; ~~Bittner et al., 2020~~; Jukić and Denić-Jukić, 2009; ~~Tritz et~~

60 ~~al., 2011~~; ~~Bittner et al., 2020~~). This approach is well suited to karst systems due to the high heterogeneity and low level of knowledge of their structure (Fleury et al., 2009; Hartmann et al., 2012). Although several authors compared the performance of different ANN models (~~Cheng et al., 2020~~; Kurtulus and Razack, 2010; Kovačević et al., 2018; ~~Cheng et al., 2020~~) and studied structure and parameters' equifinality in reservoir models (~~Makropoulos et al., 2008~~; ~~Hartmann et al., 2012~~; Gondwe et al., 2011; ~~Hartmann et al., 2012~~; ~~Mazzilli et al., 2012~~; ~~Makropoulos et al., 2008~~), only few studies have

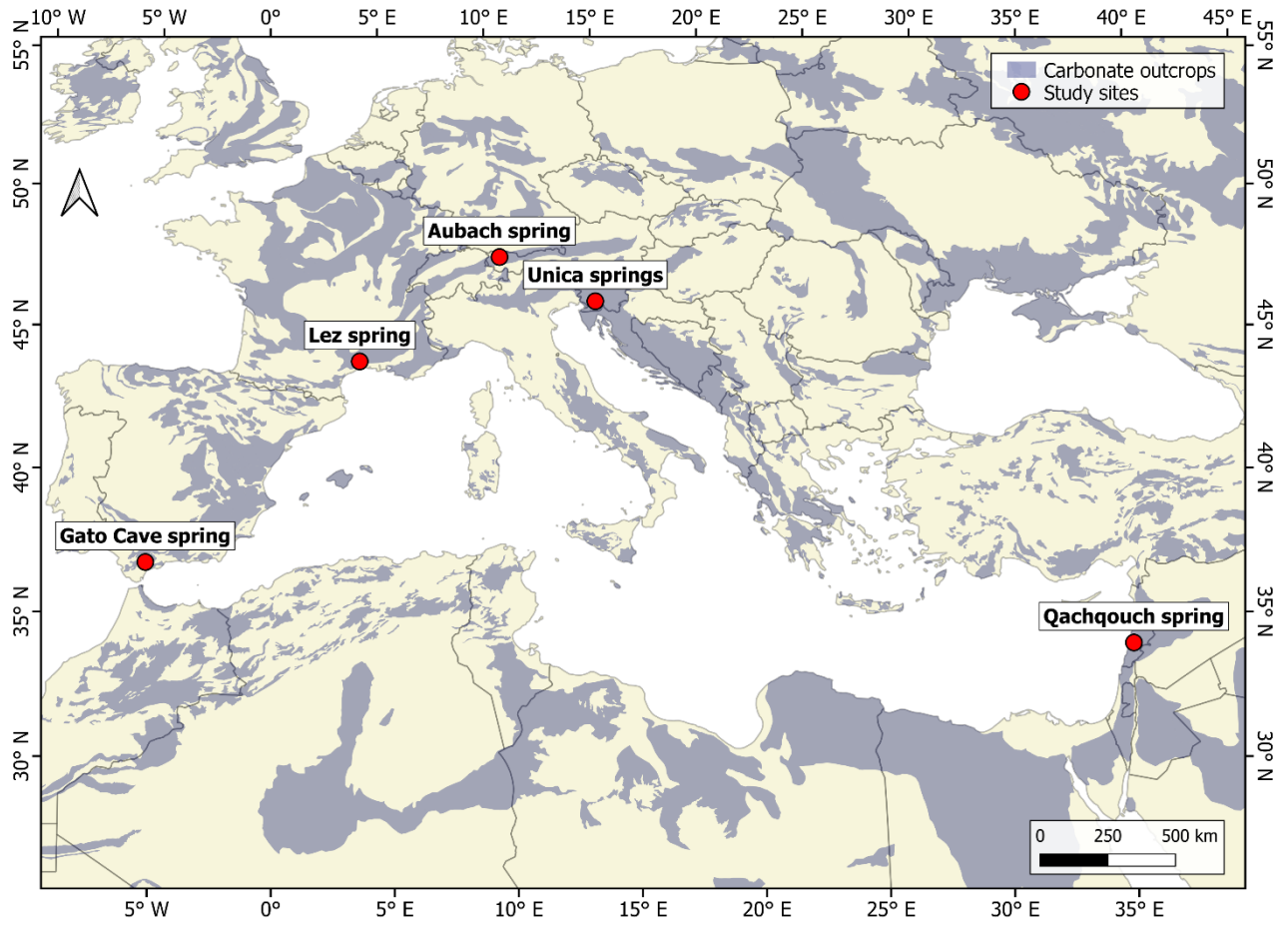
65 been conducted on the comparison of both approaches in karst environments (Jeannin et al., 2021; Kong A Siou et al., 2014; Sezen et al., 2019; Jeannin et al., 2021). Kong A Siou et al. (2014) observed that ANN models are more effective for accounting for the nonlinearity of karst systems during extreme events (dry and flood periods), while reservoir models were better for representing the hydrological functioning of the system during intermediate water periods. Sezen et al. (2019) observed that ANN models were better for simulating low-flow periods and reservoir models for simulating spring  
70 discharges on predominantly non-karst catchments. Jeannin et al. (2021) emphasised the great potential of ANN models but highlighted two main limitations: (i) they require long time series to accurately learn the functioning of a karst system, and (ii) usually no information about specific functioning of a system can be deduced from the results.

The performance of ANN and reservoir models can therefore be influenced by the characteristics of the catchment, as well as the format and length of the input data. The aim of the present study is to help researchers and stakeholders to choose  
75 between ANN and reservoir modelling approaches for simulating karst spring discharge, depending on their purpose and the available data. This research provides the first extensive comparison of ANN and reservoir models in karst hydrology by investigating results on five study sites with different context and input data. We use ANN as they have proven to be fast and reliable for modelling hydrological time series (~~Wunsch et al., 2021~~; Van et al., 2020; Jeannin et al., 2021; Wunsch et al.,  
80 2021). We specifically apply 1D Convolutional Neural Networks (CNNs) because in an earlier study (Wunsch et al., 2022) we were able to demonstrate their high ability to perform karst spring discharge modelling. Furthermore, they have some favourable properties compared to popular recurrent neural networks (e.g. the LSTMs), such as batch-wise training procedure which makes them considerably faster and computationally less expensive. Reservoir modelling is carried out using the KarstMod platform, as it provides a powerful modular interface for varying the structure, parameters and transfer functions of the conceptual model (Mazzilli et al., 2019). This research seeks to address the following research questions:

- 85
- What are the advantages and drawbacks of ANN and reservoir models in karst hydrogeology?
  - To which extent can ANN and reservoir models be used to get a better understanding of system functioning?
  - What are the implications from a stakeholder's perspective?
  - ~~Is one approach better suited for climate change predictions?~~

## 2 Data and study sites

90 We compare ANN and reservoir modelling approaches using data from five different well-studied karst systems (Table 1, Fig. A1). All systems have different characteristics in terms of hydrogeological properties (e.g. catchment area, karstification), data availability (e.g. length of the time series, number of meteorological stations, time step), and environmental conditions (e.g. climate, anthropogenic influence). Each study site is detailed in the following subsections and further details about the meteorological data can be found in Table ~~B1~~A1.



95

**Figure 1: Location of the study sites (carbonate outcrops from Goldscheider et al. (2020)).**

**Table 1: Summary of studied springs and areas.  $Q_{\text{mean}}$  corresponds to the mean observed discharge and  $P_{\text{an}}$  to the annual mean precipitation over the considered period.**

Spring	Country	Climate	Catchment area [km <sup>2</sup> ]	$Q_{\text{mean}}$ [m <sup>3</sup> .s <sup>-1</sup> ]	$P_{\text{an}}$ [mm]	Period
Aubach	Austria	Cool temperate and humid	9	0.91	2113	2012-11-20 – 2020-10-31
Gato Cave	Spain	Mediterranean	69-79	1.50	1872	1963-10-02 – 2015-04-29
Lez	France	Mediterranean	130	0.84	904	2008-10-21 – 2020-12-03
Qachqouch	Lebanon	Mediterranean	56	2.01	1293	2015-09-06 – 2020-02-05
Unica	Slovenia	Moderate continental	820	21.97	1605	1961-01-02 – 2018-12-31

## 2.1 Aubach spring, Austria

Aubach spring (1080 m asl) is a large non-permanent spring located in the Hochiften-Gottesacker area, on the border between Germany and Austria (Northern Alps). The Hochiften-Gottesacker system covers an area of about 35 km<sup>2</sup> and its altitude varies between 1000 and 2230 m asl (Chen et al., 2018). The area is under a cool temperate, humid climate and is strongly affected by snow accumulation and melting, which typically occur between November and May (Chen et al., 2018). The spring is located in the Schwarzwasser valley, which follows the geological contact between highly karstified limestone (Schrattenkalk formation) in the northern and western part and impermeable sedimentary rocks of the Flysch zone in the southern part (Goldscheider, 2005). The main catchment of Aubach spring is estimated to be approximately 9 km<sup>2</sup> (Goldscheider, 2005; Chen and Goldscheider, 2014). The spring also receives inflow from several upstream karst catchments and the Flysch zone, where surface runoff can sink into an estavelle and pass through an underground karst conduit during low-flow periods, as demonstrated by multiple tracer tests (Goldscheider, 2005).

Precipitation and temperature data were obtained from three meteorological stations located outside the catchment. The potential evapotranspiration is calculated using data from one station with the modified Turk-Ivanov approach after Wendling and Müller (1984), described in Conradt et al. (2013).

## 115 2.2 Gato Cave spring, Spain

Gato cave spring (462 m asl) is one of the main outlets of the karst system of Sierra de Libar. It is located in the north-western part of the province of Málaga, within the boundaries of the Grazalema Natural Park, about 75 km west of Málaga. The altitude of the Sierra de Libar varies between 400 and 1400 m asl according to the main north-east/south-west mountain alignments. The area is under a Mediterranean climate, with an average annual precipitation of about 1500 mm and defined by a strong seasonal pattern (Andreo et al., 2006). The site is located within the External Zone of the Betic Cordillera and presents mainly Jurassic limestones and dolomites, Cretaceous-Paleogene marly-limestones and Tertiary clays and sandstones (Flysch) that cover the whole Mesozoic rock sequence. The Jurassic rocks outcrop as anticlinal cores, while the

synclines and tectonic grabens are composed of Cretaceous rocks (Martín-Algarra, 1987). The Hundedero-Gato system constitutes a binary karst system where a wide range of well-developed karst landforms are found, such as karrenfields, swallow holes and caves. These features strongly condition recharge, which is primarily produced in two ways: (i) autochthonous, by direct infiltration of rainfall through carbonate outcrops (20-40 km<sup>2</sup>) as well as rainwater that infiltrates through swallow holes in poljes; and (ii) allochthonous, as a contribution from runoff produced in the Gaduares River basins (43.5 km<sup>2</sup>). This runoff is stored in the Montejaque dam, which was built on karstified limestone, resulting in water losses in the reservoir and, consequently, the artificial recharge of the aquifer through the Hundedero cave (Andreo et al., 2004). Precipitation and temperature data are from the meteorological station of Grazalema, which is the closest to the catchment, and therefore the most representative. Potential evapotranspiration is calculated with the Hargreaves-Samani approach (Hargreaves and Samani, 1985).

### 2.3 Lez spring, France

The Lez spring (64 m asl) is located 15 km north of Montpellier, and the altitude of its catchment varies between 64 and 655 m asl. The Lez catchment is exposed to a Mediterranean climate, which is characterised by hot, dry summers, mild winters and wet autumns. As a large part of the hydrogeological basin is relatively impermeable due to the presence of marl and marly-limestone formation, the effective recharge area of the Lez spring covers about 130 km<sup>2</sup> (Fleury et al., 2009) and corresponds to Jurassic limestone outcrops. Localized infiltration occurs through fractures and sinkholes along the basin and through the major geologic fault of Corconne-Les Matelles. The Lez aquifer is subject to anthropic pressure (i.e. exploitation for water supply) with pumping directly into the karstic conduit. The discharge is measured at the spring pool and is regularly zero during low water periods, when the pumping rate exceeds the natural discharge of the spring. Precipitation data are from four meteorological stations. Three are located in the catchment and one is located about 5 km west of the catchment. Potential evapotranspiration is calculated with the Oudin approach (Oudin et al., 2005). Temperature data are from the Prades-le-Lez meteorological station.

### 2.4 Qachqouch spring, Lebanon

Qachqouch spring (64 m asl) is located in the Nahr el-Kalb catchment and originates from a Jurassic karst aquifer. The recharge area is estimated to be about 56 km<sup>2</sup> with altitudes ranging from 60 to over 1500 m asl (Doummar and Aoun, 2018; Dubois et al., 2020). The catchment is primarily exposed to a Mediterranean climate, with snow influence at higher altitudes (Dubois et al., 2020). The lithology mainly consists in Jurassic karstified limestone and dolomitic limestone (on the higher plateaus) changing to more massive micritic limestone in the lower part of the catchment. The Qachqouch system is characterised by a duality of flow in a low permeability matrix and a high permeability conduit system (Dubois, 2017). Potential runoff inflows from higher altitudes and infiltrates downstream into the Jurassic karst aquifer. Precipitation and temperature data are from two meteorological stations. One is located in the catchment at 950 m asl. The other, with a heated rain gauge, is located 22 km north-east of the catchment at 1700 m asl (Doummar et al., 2018). Potential

155 evapotranspiration is calculated using data from the 950 m station with the modified Penman-Monteith approach (Allen et al., 1998).

## 2.5 Unica springs, Slovenia

Unica springs (450 m asl) are the outlets of a complex karst system with an estimated recharge area of about 820 km<sup>2</sup>. The area is under a moderate continental climate and is strongly influenced by snow accumulation and melting. It is subdivided into three subcatchments, with a predominance of (i) allogenic infiltration from two subcatchments drained by sinking rivers flowing through a chain of karst poljes and a river valley, and (ii) autogenous infiltration through a karst plateau with highly karstified limestone (Gabrovšek et al., 2010; Kovačič, 2010; Petric, 2010). The poljes follow each other in a descending series at altitudes between 450 and 750 m asl and are connected in a common hydrological system. Characterised by a network of surface rivers and frequent flooding, this induces a very particular response at the Unica springs with very high hydrological variability (by several orders of magnitude), as well as delayed and prolonged high-flow values (Mayaud et al., 2019). Low-flow periods are sustained by flows from the karstified limestone aquifer, which reaches heights up to 1800 m asl and has significant groundwater storage (Ravbar et al., 2012). Part of the discharge is lost due to an underground bifurcation (Kogovšek et al., 1999). When the discharge exceeds about 60 m<sup>3</sup> s<sup>-1</sup> and remains high for a few days, a polje downstream of the springs becomes flooded. When the discharge reaches about 80 m<sup>3</sup> s<sup>-1</sup>, the flooding reaches the monitoring station, influencing the measurement. The water from the lake is drained by several ponors downstream of the monitoring station, but their absorption capacity is much lower than the discharges of the springs.

Precipitation, snow cover height, and height of new snow data were obtained from two meteorological stations located on the catchment. Temperature and relative humidity data are from Postojna meteorological station only. Potential evapotranspiration is calculated using data from the Postojna station with the modified Penman-Monteith approach (Allen et al., 1998).

## 3 Methodology

### 3.1 Artificial neural networks

ANN are a branch of Machine Learning, i.e. a technique to learn complex relations from existing data. They imitate the basic functioning of biological nervous systems and similarly consist of mathematical representations of neurons structured and interconnected in layers. Given sufficient data from which to learn, ANN can establish complex input-output relations with only limited domain knowledge.

In this study, ~~Convolutional Neural Networks (CNN)~~CNNs (LeCun et al., 2015) – a specific model type from the ANN-subfield of Deep Learning (DL) – ~~were~~is used. CNNs are predominantly successful in processing image-alike data, but are also useful in signal processing for sequential data. They usually consist of sequences or blocks of convolutional layers for feature recognition and pooling layers for information consolidation. In the former, filters of a specific size (defining their

receptive field) are used to produce feature maps. These feature maps are subsequently down-sampled (often by maximum selection) into pooling layers to consolidate the contained information. Several of these blocks with varying properties can be stacked on top of each other, also in combination with other layer types such as batch normalization layers (Ioffe and Szegedy, 2015) to prevent exploding gradients or dropout layers (Srivastava et al., 2014). Lastly, one (or multiple) fully connected dense layers follow to produce the model output. For the models in this study, we used a single 1D-Convolutional layer with a fixed kernel size (three) and an optimised number of filters. This layer was succeeded by (i) a Max-Pooling layer, (ii) a Monte-Carlo dropout layer (10 % dropout rate) and (iii) two dense layers: the first with an optimised number of neurons and the second with a single output neuron (Fig. 2). Besides number of filters and number of neurons in the first dense layers, we optimised the training batch size and the length of the input sequence for each simulation step using the Bayesian Optimization library (Nogueira, 2014). The number of minimum and maximum optimisation steps was individually selected for each site and can be found in the provided modelling scripts (Cinkus and Wunsch, 2022). To ensure proper learning, the models are regularised with several measures. Hence, early stopping with a patience of 20 steps is applied to prevent the model from overfitting. Except Qachqouch, where little data is available, the size of the according stopset ranges between one and four annual cycles (see provided scripts for details). This stopset is considered a part of the calibration period mentioned in Sect. 3.4. Further, dropout ensures robust training and serves as another measure against overfitting. We applied the Adam optimizer for a maximum of 150 to 300 training epochs with an initial learning rate of 0.001 and applied gradient clipping to prevent exploding gradients. We programmed our models in Python 3.8 (van Rossum, 1995), using the following frameworks and libraries: Numpy (van der Walt et al., 2011), Pandas (Reback et al., 2021; McKinney, 2010), Scikit Learn (Pedregosa et al., 2018), Matplotlib (Hunter, 2007), BayesOpt (Nogueira, 2014), TensorFlow 2.7 (Abadi et al., 2016) and its Keras API (Chollet et al., 2015).

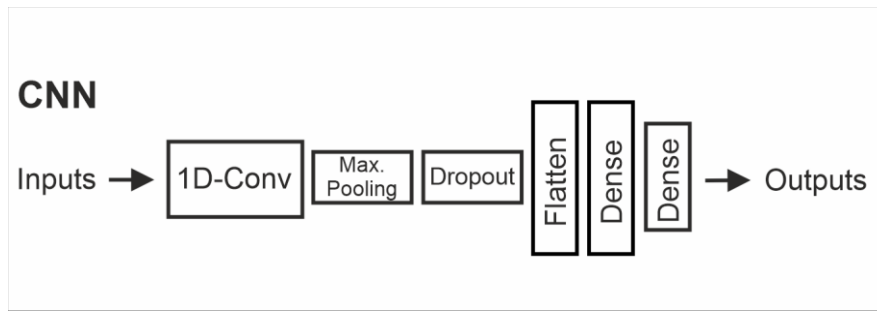


**Figure 2: Selected structure of the CNN model.**

### 3.2 Reservoir models

Reservoir models are a conceptual representation of a hydrosystem, which involves the association of several reservoirs that are thought to be representative of the main processes at stake. Each reservoir is characterised by its water height and a flow equation that translates the variations of water height into discharges. The flow equation is function of a specific discharge

coefficient and a positive exponent (different from 1 for non-linear flows), which are defined by calibration against observed data.

215 Many reservoir models have been developed to study the relation between precipitation and discharge in karst systems (Hartmann et al., 2014). They all differ in complexity with respect to the number of reservoirs and parameters, which need to be well thought out in order to preserve physical realism and limit equifinality on model parameters. Careful sensitivity analyses and uncertainty assessment should be considered along with model results to avoid over-interpretation (Refsgaard et al., 2007). Reservoir models can be seen as a compromise between simulation performance and insight into the functioning of a system. ~~This approach is well suited to karst systems due to the high heterogeneity and low level of knowledge of their structure (Hartmann et al., 2012; Fleury et al., 2009).~~

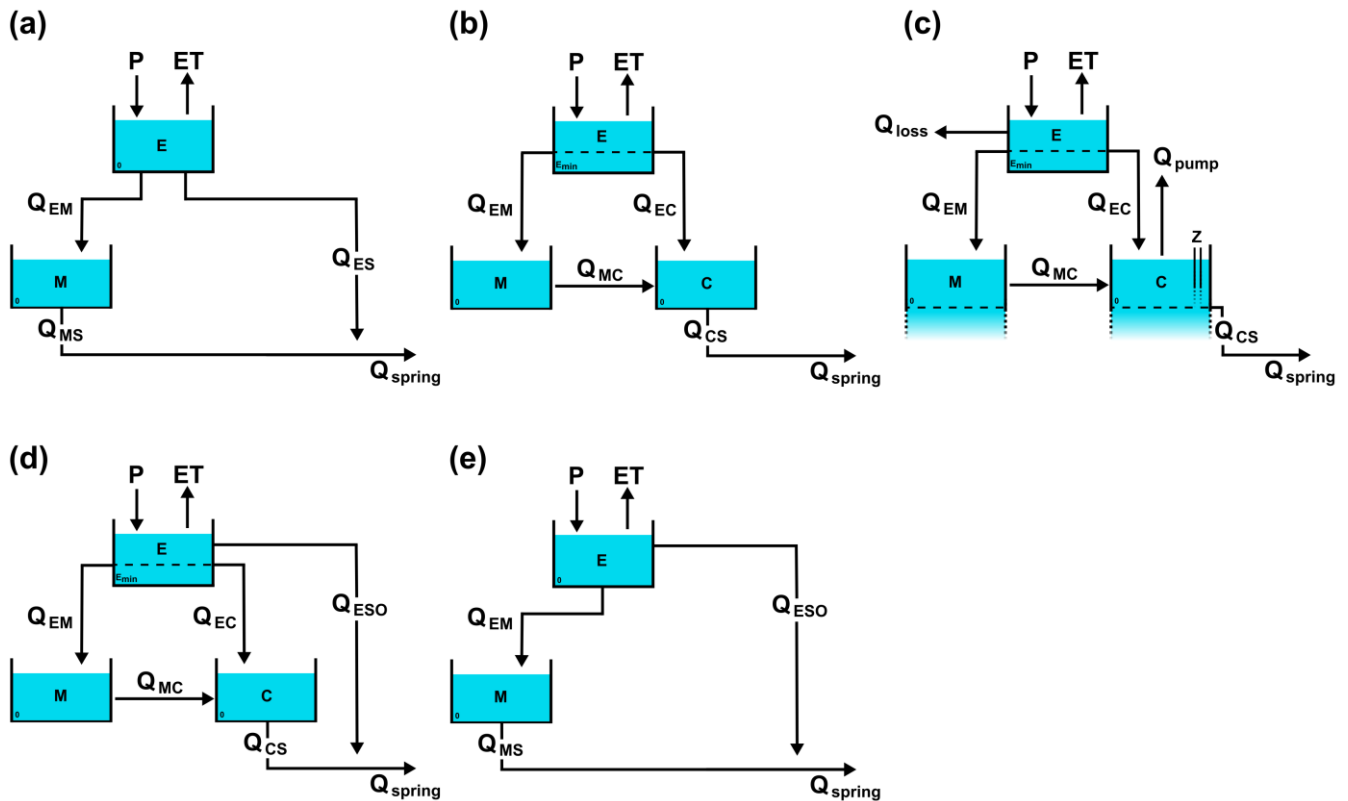
220 We used the adjustable modelling platform KarstMod for performing reservoir modelling. KarstMod provides a modular, user-friendly interface for simulating spring discharge at karst outlets. Structure of models built using [the](#) KarstMod platform is based on the conceptual model of a karst aquifer with infiltration and saturated zones (Mazzilli et al., 2019). The infiltration zone (soil and epikarst) drains water from the surface through a vertical network of fissures and conduits. Water storage can occur in the unsaturated zone, as well as local saturation. The saturated zone comprises a dual porosity functioning, with a network of high-permeability fractures and conduits, and a low-permeability matrix with a high storage capacity.

225 In KarstMod, the model structure can include up to four reservoirs. One at the upper level reflects the processes (infiltration, storage and drainage) occurring in the soil and epikarst zone. Three at the lower level can be connected with the first one and correspond to the infiltration and/or saturated zones. The discharge can be simulated with (i) several linear and non-linear water level-discharge laws, (ii) a hysteretic water level-discharge function to reproduce the hysteretic functioning observed on the wet-dry cycles in the unsaturated zone (Lehmann et al., 1998; Tritz et al., 2011), and (iii) an exchange function that aims to reproduce the interactions between matrix and conduits. More details on the balance equations, the parameters involved and the KarstMod platform in general can be found in Mazzilli et al. (2019) or in the KarstMod User Guide (Mazzilli and Bertin, 2019).

230 In this study, we first addressed the structure of the models taking into account our expert knowledge and previous studies. For each site, we examined the major characteristics that determine the functioning of the system and associated the corresponding conceptual modelling. We then modified this base structure according to the performance of the model while trying to maintain physical realism. The most efficient model structures that we obtained after performing the modelling are shown in Fig. [3+1](#).

240 Aubach spring selected model (Fig. [3+1a](#)) is close to the conceptual model with a very reactive transfer function ( $Q_{ES}$ ), corresponding to the well-developed conduit network, and a matrix reservoir (M), which in this case mostly reflects the storage properties in the unsaturated limestone. We tested different configurations (lost discharge from upper level reservoir and/or pumping in lower reservoirs) to simulate the lost discharges through overflow springs and underground flows, but there were no significant increases in model performance. Gato Cave spring selected model (Fig. [4b3b](#)) is different from the

conceptual model as the platform could not account for the allochthonous recharge on the catchment. The model structure includes a soil available water capacity ( $E_{min}$ ), matrix and conduits compartments (M and C), as well as matrix-conduits exchanges ( $Q_{MC}$ ), which may translate the processes occurring through the dam. Lez spring selected model (Fig. 43c) is accurate with the conceptual model and includes an overflow transfer function ( $Q_{loss}$ ), matrix and conduits compartments (M and C), matrix-conduits exchanges ( $Q_{MC}$ ), and pumping into the main conduit ( $Q_{pump}$ ). We considered a low soil available water capacity ( $E_{min}$ ) as it greatly increased the performance of the model. Qachqouch spring selected model (Fig. 43d) is consistent with previous conceptual models that considered many different response times. The model structure features a very reactive transfer function ( $Q_{ESO}$ ), matrix and conduits compartments (M and C), matrix-conduits exchanges ( $Q_{MC}$ ) as well as a soil available water capacity. The multiple different transfer functions help to reproduce the reactive and dampened responses of the Qachqouch karst aquifer. Unica springs selected model (Fig. 43e) is significantly simpler than the conceptual model, which includes polje flooding, allochthonous recharge, overflow springs and matrix-conduits exchanges. We only retained a very simple structure as it was the best trade-off between physical realism and model performance. The very reactive transfer function  $Q_{ESO}$  allows reproducing fast flows through conduits, while the matrix reservoir (M) likely translates processes occurring in the matrix and surface flooding.



260

Figure 43: Selected model structures for (a) Aubach, (b) Gato Cave, (c) Lez, (d) Qachqouch and (e) Unica springs. Flux names correspond to the terminology of the KarstMod platform (Mazzilli and Bertin, 2019).

### 3.3 Input data

Input data are the time series that are used for simulating karst spring discharge. They can be derived from either a direct observation (e.g. observed discharge, temperature, sinking stream discharge or pumping) or a calculation from raw input data (e.g. potential evapotranspiration derived from temperature). Nature of input data usually differs between ANN and reservoir modelling approaches, as ANN models tends to make good use of direct observations, whereas reservoir models often requires to preprocess the raw input data. We decided to work with raw input data to ensure equitable performance between ANN and reservoir models. The raw input data was either used directly or preprocessed, depending on the modelling approach.

The data used for each modelling approach and site is summarised in Table 2. Observed discharge time series were used directly (without further preprocessing) in ANN and reservoir models. In the case of the Lez spring, the models were simultaneously calibrated on the spring discharge ( $Q$ ) as well as on the water level in the aquifer ( $Z$ ). Furthermore, the pumped discharge time series in reservoir C ( $Q_{\text{pump}}$ , Fig. 4e3c) was used as an input. Precipitation time series were used differently as there are often several meteorological station per study site. For ANN models, precipitation time series were used as raw input  $P_{\text{raw}}$ , except for Lez spring where the individual raw precipitation data had too many missing values so we used the same input as the reservoir model ( $P_{\text{in}}$ ). In the case of Aubach, Qachqouch and Unica,  $P_{\text{raw}}$  includes all the precipitation time series from the different meteorological stations (Table B4A1). For reservoir models, the precipitation time series were either (i) used directly if there was no snow dynamics on the catchment and only one meteorological station was available (Gato Cave), (ii) preprocessed with Thiessen’s polygons interpolation (Appendix CB) if there were several meteorological stations (Lez), (iii) preprocessed with a snow routine (Appendix DC) to simulate snow accumulation and melting over the catchment (Aubach) if snow dynamics could not be neglected, or (iv) preprocessed with both Thiessen’s polygons interpolation and snow routine (Qachqouch, Unica). For reservoir models, evapotranspiration processes were considered using time series of potential evapotranspiration, which were calculated for each site using different methods depending on the available meteorological data, the climate of the area and local expert knowledge. For ANN models, we used temperature time series instead of evapotranspiration because calculating potential evapotranspiration is generally not necessarily beforehand. Additionally, we used a sinusoidal temperature signal time series ( $T_{\text{sin}}$ , derived from the observed temperature) to better account for seasonality in Aubach, Lez and Unica ANN models.

**Table 2: Summary of input data.** (i)  $P_{\text{raw}}$ , (ii)  $P_{\text{in}}$  and (iii)  $P_{\text{sr}}$  refer to (i) raw precipitation data, (ii) precipitation data interpolated with Thiessen’s polygons method, and (iii) precipitation data redistributed by applying the snow routine.  $Q_{\text{obs}}$ ,  $Z_{\text{obs}}$  and  $T$  refer to observed discharge, observed water level and temperature, respectively. ET (Evapotranspiration) refers to either PET (Potential Evapotranspiration) or AET (Actual Evapotranspiration) time series.

Spring	Time step	Date Range	Data used				Maximum gap [days]			
			ANN	Reservoir			P	T	Q	ET

Spring	Time step	Date Range	Data used		Maximum gap [days]			
			ANN	Reservoir	P	T	Q	ET
Aubach	Hourly	2012–2020	$Q_{obs}, P_{raw}, T, T_{sin}^a$	$Q_{obs}, P_{sr}, PET^c$	0	0	0	0
Gato Cave	Daily	1963–2015	$Q_{obs}, P_{raw}, T_{max}, T_{min}, T_{med}$	$Q_{obs}, P_{raw}, PET$	0	0	0	0
Lez	Daily	2008–2020	$Q_{obs}, Q_{pump}, Z_{obs}, P_{in}, T_{sin}$	$Q_{obs}, Q_{pump}, Z_{obs}, P_{in}, PET$	0	2	7	0
Qachqouch	Daily	2015–2020	$Q_{obs}, P_{raw}, T_{max}^b$	$Q_{obs}, P_{in}, PET$	0	0	11	0
Unica	Daily	1961–2018	$Q_{obs}, P_{raw}, T, T_{sin}, NS$	$Q_{obs}, P_{in-sr}, PET$	0	1	0	29

<sup>a</sup> $P_{raw}, T$  and  $T_{sin}$  data are from Diedamskopf, Oberstdorf and Walmendinger Horn meteorological stations

<sup>b</sup> $T_{max}$  data are from the 1700 m meteorological station

<sup>c</sup> $P_{sr}$  data are calculated with the data from Diedamskopf station

We handled missing values in the different time series as follows: (i) temperature gaps were linearly interpolated, (ii) precipitation and evapotranspiration gaps were considered to be equal to 0, and (iii) discharge gaps were interpolated with a Lagrange polynomial function. Maximum observed gaps for precipitation, temperature, discharge and evapotranspiration time series are detailed in Table 2. Note that (i) for Lez spring, we observed maximum gaps of 17 and 16 days for pumped discharge and piezometric level, respectively; and (ii) for Unica springs, there are no missing values in the Cerknica new snow height (NS) time series.

### 3.4 Model calibration and simulation

The calibration period is the period used for selecting the parameters that provide the best results according to the performance measure. The validation period is intended to assess the relevance of the parameters over a time interval that is not used for calibration. In the domain of the ANN modelling, the validation is usually denoted as testing period. However, we unify the terminology at this point. The calibration period is again split into three different parts in the case of ANN modelling, (i) to train the model, (ii) to prevent the model from overfitting, and (iii) to optimize its hyperparameters. We defined the same calibration and validation periods for both modelling approaches (Table 3), which ensures fair initial conditions and a meaningful comparison of the results. We have chosen the periods in a way to maximise the length of the calibration periods, which allows for relevant model results (especially in ANN models). In reservoir model, we considered a short warm-up interval at the beginning of the calibration period for the model to adjust and reach an optimal state.

**Table 3: Calibration and validation periods.**

Spring	Calibration period	Validation period	Objective function
--------	--------------------	-------------------	--------------------

					ANN	Reservoir
Aubach	2014-04-18	2019-12-31	2020-01-01	2020-10-31	MSE(Q)	NSE(Q)
Gato Cave	1963-10-02	2011-09-03	2011-09-04	2015-04-29	MSE(Q)	NSE(Q)
Lez	2008-10-21	2017-12-31	2018-01-01	2020-12-03	MSE(Q, Z)	NSE(Q, Z)
Qachqouch	2015-09-06	2019-09-30	2019-10-01	2020-01-22	MSE(Q)	NSE(Q)
Unica	1961-01-02	2016-09-28	2016-09-29	2018-12-31	MSE(Q)	NSE(Q)

**Table 3: Calibration and validation periods.**

Spring	Calibration period	Validation period	Objective function
Aubach	2014-04-18 – 2019-12-31	2020-01-01 – 2020-10-31	MSE(Q)
Gato Cave	1963-10-02 – 2011-09-03	2011-09-04 – 2015-04-29	MSE(Q)
Lez	2008-10-21 – 2017-12-31	2018-01-01 – 2020-12-30	MSE(Q, Z)
Qachqouch	2015-09-06 – 2019-09-30	2019-10-01 – 2020-01-22	MSE(Q)
Unica	1961-01-02 – 2016-09-28	2016-09-29 – 2018-12-31	MSE(Q)

315 We calibrated the models by applying the Mean Squared Error (MSE) ~~and the Nash-Sutcliffe Efficiency (NSE, Nash and~~  
~~Sutcliffe (1970)) criteria in ANN and reservoir models, respectively~~ on simulated and observed discharges time series.  
For Lez spring, we used a composite function of discharge and water level in order to consider both variables in the same  
modelling process.

320 ~~A total of 1000~~Multiple simulations were carried out for each modelling approach at each site. The obtained simulated  
discharge (or water level) time series corresponds to the mean of the distribution of simulated values at each time step. We  
also considered the uncertainties in the model prediction by calculating the 90 % confidence interval, whose limits  
correspond to the 0.05 and 0.95 quantile of the distribution at each time step.

325 In KarstMod (reservoir models), the retained simulations correspond ~~to the 1000 best results of a one-hour simulation run to~~  
~~all the results satisfying a maximum MSE threshold on the calibration period for a 6-hour model run.~~ The confidence interval  
reflects the uncertainty in the parameters used in the model, which are not fixed but defined as a range (e.g. catchment area =  
150 to 200 km<sup>2</sup>). In the case of ANN models, we used a model ensemble of 10 models based on different random number  
generator seeds for model initialization. Using the Monte-Carlo dropout layer, for each of the ensemble members a total of  
100 simulation results were generated.

### 3.5 Model evaluation

330 We evaluated the performance of the models using the MSE and several performance criteria that assess different aspects of  
the discharge: modified Kling-Gupta Efficiency (KGE'), KGE' components ( $r, \gamma, \beta$ ) (Kling et al., 2012) and Diagnostic  
Efficiency (DE) (Schwemmler et al., 2021). These criteria were all applied to the whole discharge regime, but also to sub-  
regimes of high- and low-flow conditions (with the exception of DE, which already takes sub-regimes into account). For Lez  
spring, we also applied the MSE and KGE' ~~eriterion-criteria~~ on water level. Model performance is usually evaluated on both  
335 calibration and validation periods for reservoir models. However, this approach is not suited to ANN models, for which the  
calibration period corresponds to the learning period of the model. Thus, we chose to only evaluate and compare the  
reservoir and ANN models on their validation periods.

The Kling-Gupta Efficiency (KGE) has gained in popularity as it aims to address some limitations of the Nash-Sutcliffe  
Efficiency (Nash and Sutcliffe, 1970), i.e. (i) the discharge variability is underestimated, (ii) the mean of observed values is  
340 not a meaningful benchmark for variables with high variability, and (iii) the normalised bias is dependent to the variability  
(Gupta et al., 2009, Willmott et al., 2012). The KGE' is based on the Kling-Gupta Efficiency KGE (Gupta et al., 2009) and  
aims to ensure that bias and variability are not cross-correlated by using the coefficient of variation ratio ( $\gamma$ ) instead of the  
standard deviation ratio ( $\alpha$ ):

$$KGE' = 1 - \sqrt{(r - 1)^2 + (\gamma - 1)^2 + (\beta - 1)^2} \quad (1)$$

345

With  $r$  the Pearson correlation coefficient between the simulated and observed discharge,  $\beta$  the ratio between mean  
simulated and mean observed discharge, and  $\gamma$  the ratio between simulated and observed coefficient of variation of  
discharge. The three components of KGE' help to evaluate different aspects of a model: (i)  $r$  is related to shape and timing  
(Santos et al., 2018), (ii)  $\beta$  is used to assess the overall volume of water discharged at the spring (further referred to as  
350 "volume"), and (iii)  $\gamma$  gives insight into the flow variability. The KGE' and  $r$  criteria can range from  $-\infty$  to 1, whereas  $\gamma$  and  
 $\beta$  can range from  $-\infty$  to  $\infty$ . A KGE' score equal to 1 means a perfect match between simulated and observed discharge,  
while a score lower than -0.41 indicates that the model is worse than using the observed mean as a predictor (Knoben et al.,  
2019).

The DE criterion is intended to help defining the weaknesses of a model. It is based on constant, dynamic and timing errors.  
355 DE is proposed as a numerical measure (ranging from 0 to  $\infty$ , with 0 indicating a perfect model), but can also be visualized  
on a polar plot that effectively differentiate error contributions. The overall error is calculated with the following equation:

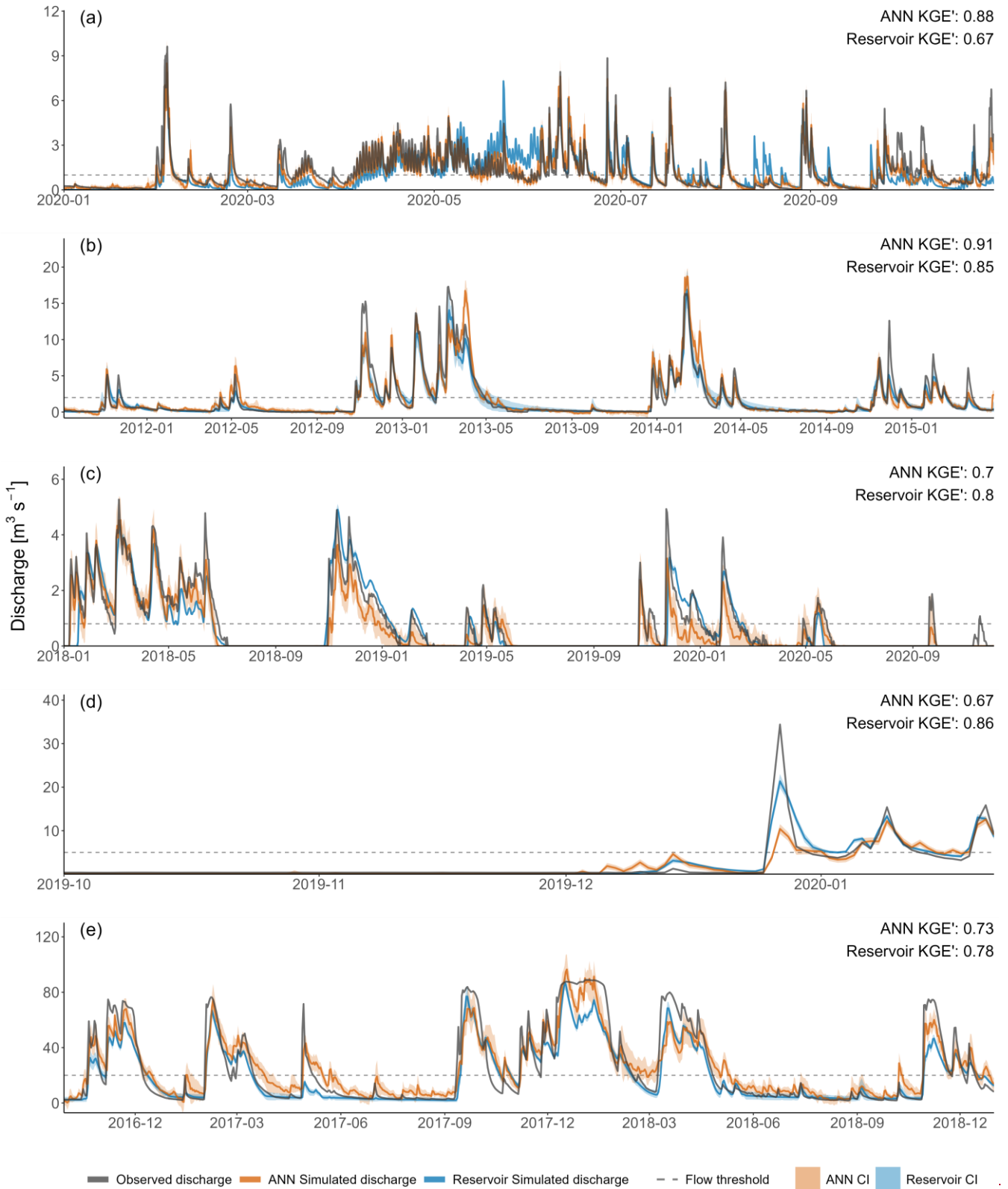
$$DE = \sqrt{B_{rel}^{-2} + |B_{area}|^2 + (r - 1)^2} \quad (2)$$

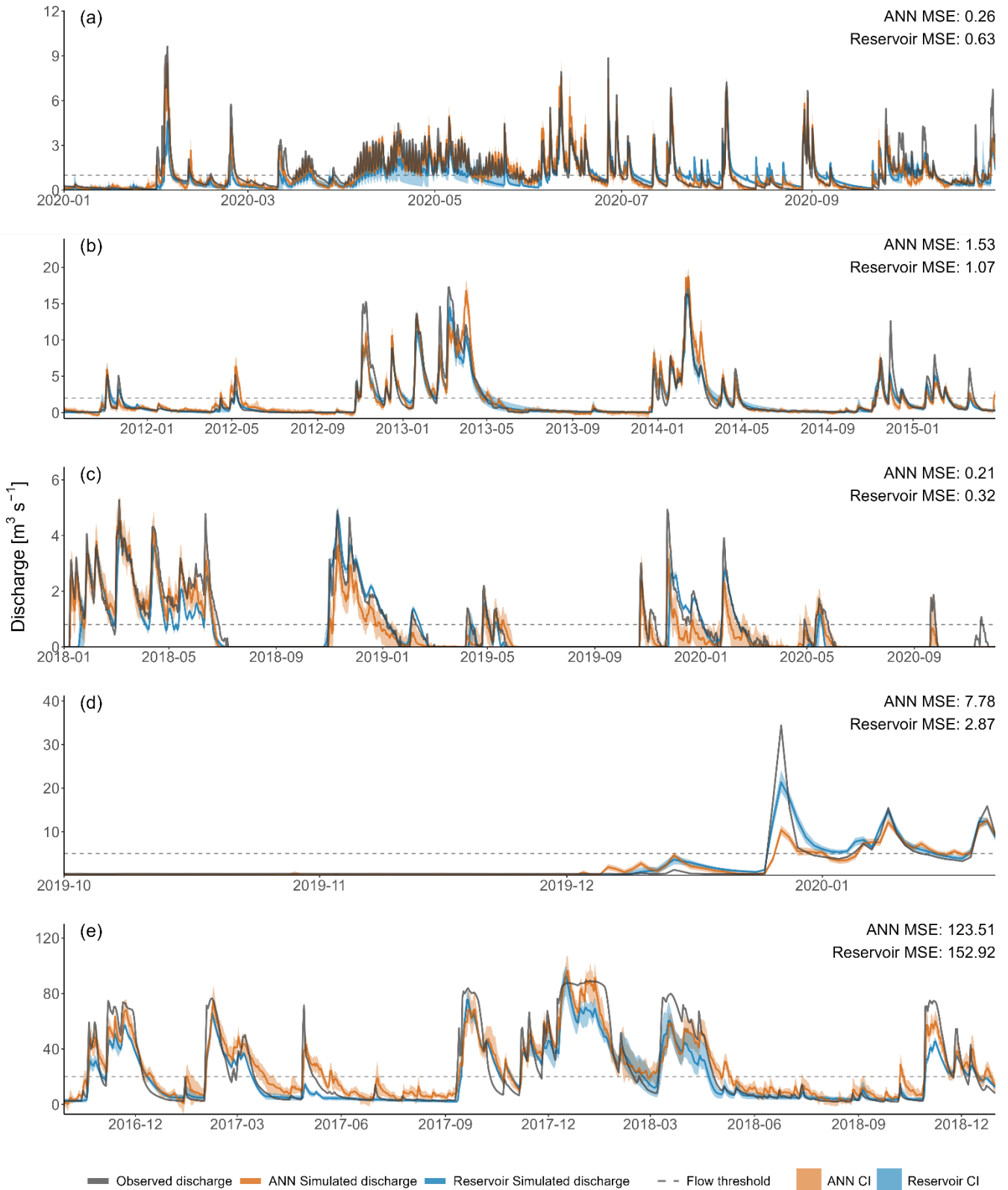
With  $\overline{B_{rel}}$  and  $|B_{area}|$  the measures for constant and dynamic errors, respectively. As these measures are based on the flow duration curve, they give an information in terms of exceedance probability. Details of their calculation can be found in Schwemmler et al. (2021).

365 The performance criteria applied to high- and low-flow conditions are denoted by the lower script indices “L” and “H”, respectively. These criteria allow the performance of the models to be evaluated over different flow regimes (i.e. dry/intermediate, wet). Discharge thresholds were set manually based on our knowledge of the system and a careful assessment of the distribution of discharge values. They are equal to 1, 2, 0.8, 5, and 20 m<sup>3</sup> s<sup>-1</sup> for Aubach, Gato Cave, Lez, Qachqouch and Unica springs, respectively.

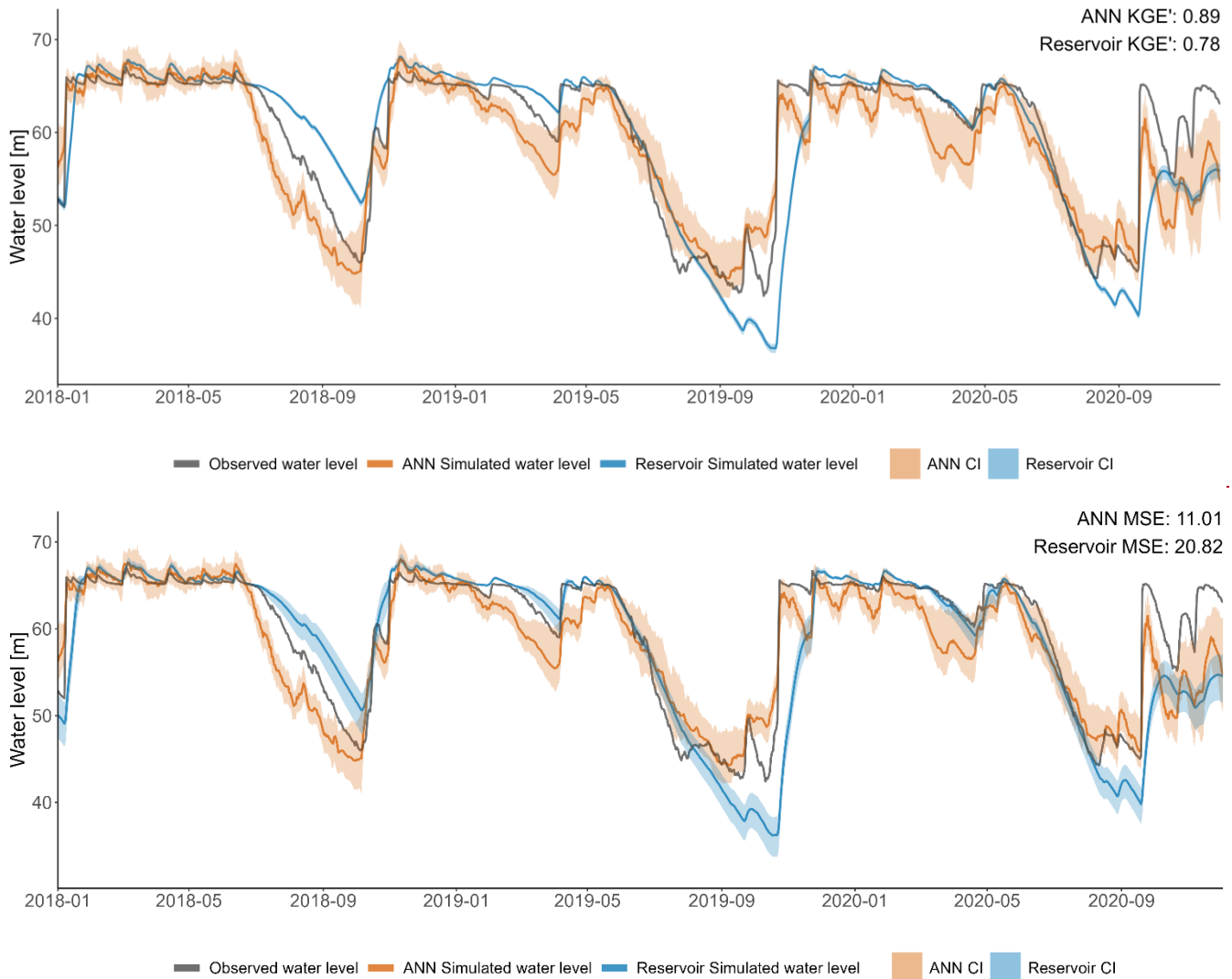
#### 4 Results and discussion

370 The obtained models and their confidence intervals for the two approaches and each test site are presented in Fig. 2-4 for discharge and Fig. 3-5 for water level (Lez spring). Their performance – assessed with multiple criteria – are shown in Fig. 4-6, and in Table 4, and Table D1. The DE polar plots for each site are presented in Fig. 5-7.

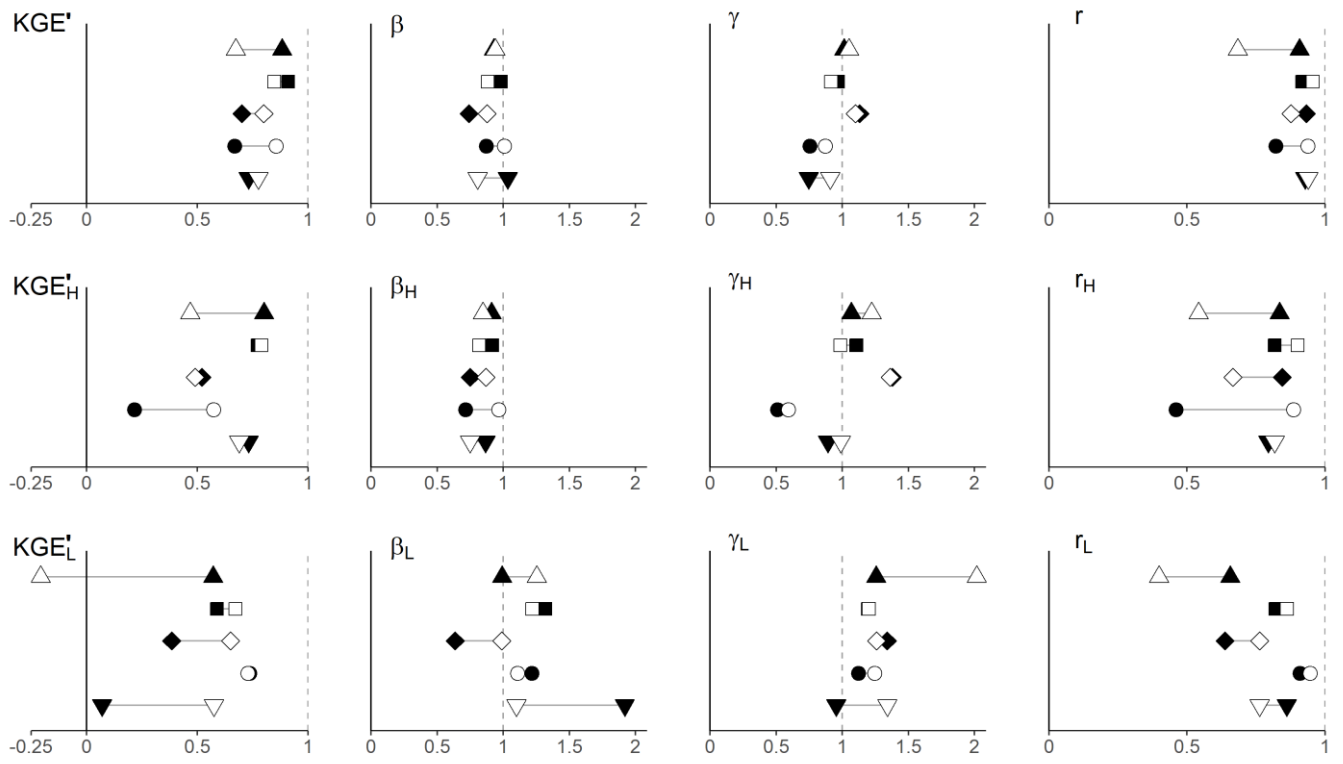




375 **Figure 24:** Observed and simulated spring discharge time series with (i) 90 % confidence intervals (CI) on the validation period and (ii) threshold for high and low flows used for the calculation of the performance criteria. (a) Aubach, (b) Gato Cave, (c) Lez, (d) Qachqouch and (e) Unica springs.



380 **Figure 35:** Observed and simulated spring water level time series with 90 % confidence intervals (CI) on the validation period (Lez spring).



	Aubach	Gato Cave	Lez	Qachqouch	Unica
ANN	▲	■	◆	●	▼
Reservoir	△	□	◇	○	▽

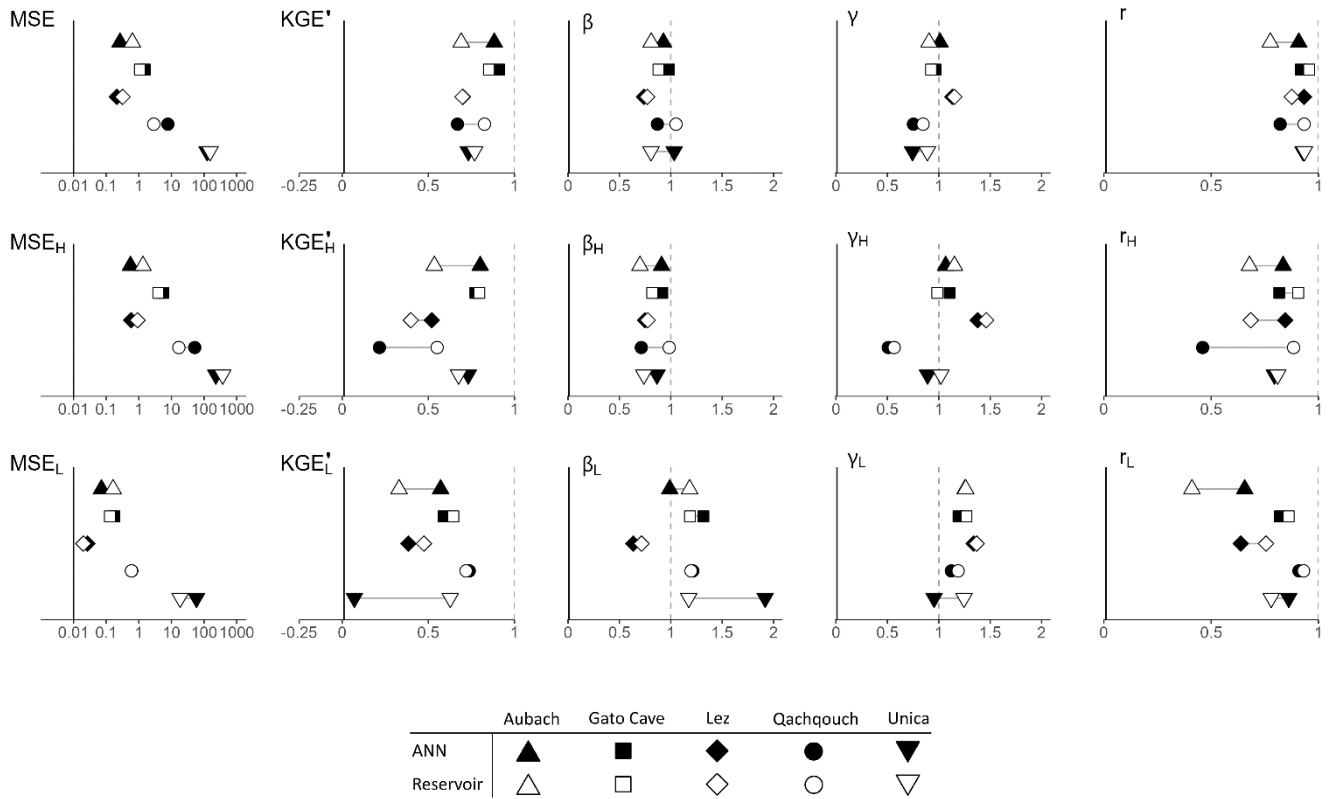


**Figure 46:** Performance of the ANN and reservoir models on the validation period, according to different performance criteria. Exact values can be found in Table 4.

**Table 4: Details of indicator values for the reservoir and ANN models on the validation period. For each site, the simulations are evaluated with different performance criteria on total, high- and low-flow conditions. Values in bold correspond to the better score between ANN and reservoir models.**

Spring	Flow regime	KGE'		$\beta$		$r$		$\gamma$	
		ANN	Reservoir	ANN	Reservoir	ANN	Reservoir	ANN	Reservoir
Aubach	Total	<b>0.88</b>	0.67	0.93	<b>0.94</b>	<b>0.91</b>	0.68	<b>1.01</b>	1.05
	High flow	<b>0.80</b>	0.47	<b>0.91</b>	0.85	<b>0.84</b>	0.54	<b>1.07</b>	1.22
	Low flow	<b>0.57</b>	-0.21	<b>0.99</b>	1.25	<b>0.66</b>	0.40	<b>1.26</b>	2.01
Gato-Cave	Total	<b>0.91</b>	0.85	<b>0.98</b>	0.88	0.92	<b>0.95</b>	<b>0.97</b>	0.91
	High flow	0.77	<b>0.79</b>	<b>0.92</b>	0.82	0.82	<b>0.90</b>	1.11	<b>0.98</b>
	Low flow	0.59	<b>0.67</b>	1.32	<b>1.22</b>	0.82	<b>0.86</b>	<b>1.19</b>	1.20
Lez	Total	0.70	<b>0.80</b>	0.74	<b>0.88</b>	<b>0.93</b>	0.88	1.13	<b>1.10</b>
	High flow	<b>0.52</b>	0.49	0.75	<b>0.87</b>	<b>0.84</b>	0.67	1.38	<b>1.36</b>
	Low flow	0.38	<b>0.65</b>	0.64	<b>0.99</b>	0.64	<b>0.76</b>	1.34	<b>1.26</b>
Qachqouch	Total	0.67	<b>0.86</b>	0.87	<b>1.01</b>	0.82	<b>0.94</b>	0.75	<b>0.87</b>
	High flow	0.22	<b>0.57</b>	0.71	<b>0.96</b>	0.46	<b>0.89</b>	0.51	<b>0.59</b>
	Low flow	<b>0.74</b>	0.73	1.21	<b>1.11</b>	0.91	<b>0.95</b>	<b>1.12</b>	1.24
Unica	Total	0.73	<b>0.78</b>	<b>1.03</b>	0.80	0.93	<b>0.94</b>	0.74	<b>0.91</b>
	High flow	<b>0.73</b>	0.69	<b>0.87</b>	0.75	0.79	<b>0.82</b>	0.89	<b>0.99</b>
	Low flow	0.07	<b>0.57</b>	1.92	<b>1.10</b>	<b>0.86</b>	0.76	<b>0.95</b>	1.34

**Table 4: Details of indicator values for the reservoir and ANN models on the validation period. For each site, the simulations are evaluated with different performance criteria on total, high- and low-flow conditions. Values in bold correspond to the better score between ANN and reservoir models.**

Spring	Flow regime	MSE		KGE'		$\beta$		$r$		$\gamma$	
		ANN	Reservoir								
Aubach	Total	<b>0.26</b>	0.63	<b>0.88</b>	0.69	<b>0.93</b>	0.81	<b>0.91</b>	0.78	<b>1.01</b>	0.91
	High flow	<b>0.55</b>	1.34	<b>0.80</b>	0.53	<b>0.91</b>	0.70	<b>0.84</b>	0.68	<b>1.07</b>	1.15
	Low flow	<b>0.07</b>	0.16	<b>0.57</b>	0.33	<b>0.99</b>	1.18	<b>0.66</b>	0.41	1.26	1.26

Spring	Flow regime	MSE		KGE'		$\beta$		r		$\gamma$	
		ANN	Reservoir	ANN	Reservoir	ANN	Reservoir	ANN	Reservoir	ANN	Reservoir
Gato Cave	Total	<u>1.53</u>	<u>1.07</u>	<u>0.91</u>	<u>0.85</u>	<u>0.98</u>	0.88	<u>0.92</u>	<u>0.96</u>	<u>0.97</u>	<u>0.92</u>
	High flow	<u>5.62</u>	<u>3.93</u>	<u>0.77</u>	<u>0.80</u>	<u>0.92</u>	0.82	<u>0.82</u>	<u>0.91</u>	<u>1.11</u>	<u>0.99</u>
	Low flow	<u>0.18</u>	<u>0.13</u>	<u>0.59</u>	<u>0.64</u>	<u>1.32</u>	<u>1.19</u>	<u>0.82</u>	<u>0.86</u>	<u>1.19</u>	<u>1.27</u>
Lez	Total	<u>0.21</u>	0.32	<u>0.70</u>	<u>0.70</u>	0.74	<u>0.77</u>	<u>0.93</u>	0.88	<u>1.13</u>	<u>1.15</u>
	High flow	<u>0.58</u>	0.92	<u>0.52</u>	<u>0.40</u>	<u>0.75</u>	<u>0.78</u>	<u>0.84</u>	<u>0.68</u>	<u>1.38</u>	<u>1.46</u>
	Low flow	<u>0.03</u>	<u>0.02</u>	<u>0.38</u>	<u>0.47</u>	0.64	<u>0.72</u>	0.64	<u>0.76</u>	<u>1.34</u>	<u>1.39</u>
Qachqouch	Total	<u>7.78</u>	<u>2.87</u>	<u>0.67</u>	<u>0.83</u>	0.87	<u>1.05</u>	0.82	<u>0.93</u>	<u>0.75</u>	<u>0.85</u>
	High flow	<u>51.74</u>	<u>16.84</u>	<u>0.22</u>	<u>0.55</u>	<u>0.71</u>	<u>0.98</u>	0.46	<u>0.88</u>	<u>0.51</u>	<u>0.57</u>
	Low flow	<u>0.61</u>	<u>0.60</u>	<u>0.74</u>	<u>0.72</u>	<u>1.21</u>	<u>1.20</u>	<u>0.91</u>	<u>0.93</u>	<u>1.12</u>	<u>1.19</u>
Unica	Total	<u>123.51</u>	<u>152.92</u>	<u>0.73</u>	<u>0.77</u>	<u>1.03</u>	0.81	<u>0.93</u>	<u>0.93</u>	<u>0.74</u>	<u>0.89</u>
	High flow	<u>229.00</u>	<u>371.37</u>	<u>0.73</u>	<u>0.68</u>	<u>0.87</u>	0.74	<u>0.79</u>	<u>0.81</u>	<u>0.89</u>	<u>1.02</u>
	Low flow	<u>58.55</u>	<u>18.43</u>	<u>0.07</u>	<u>0.63</u>	<u>1.92</u>	<u>1.17</u>	<u>0.86</u>	<u>0.78</u>	<u>0.95</u>	<u>1.25</u>

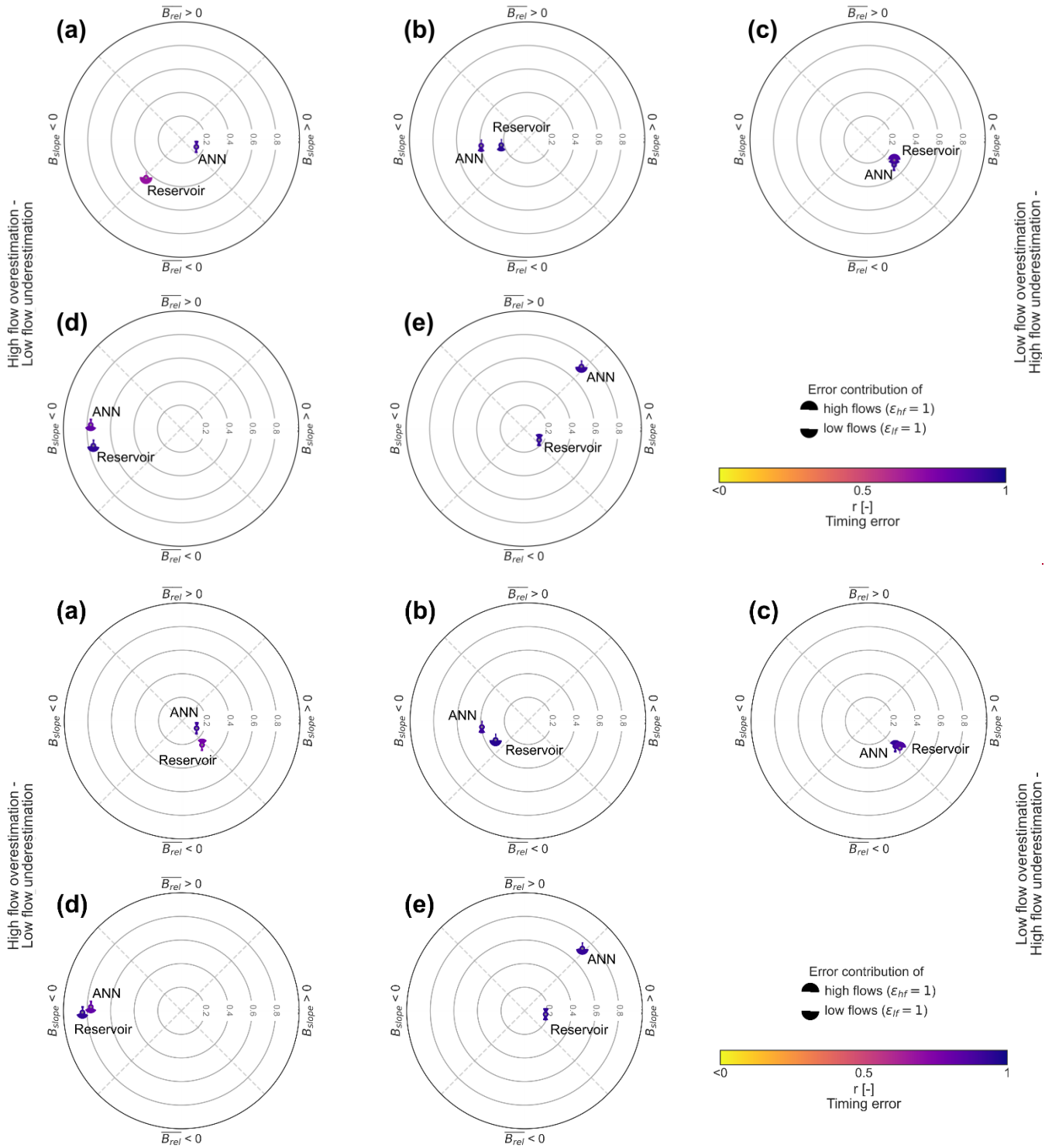


Figure 57: Diagnostic efficiency polar plots on the validation period. (a) Aubach, (b) Gato Cave, (c) Lez, (d) Qachqouch and (e) Unica springs.

## 4.1 Modelling results

### 400 4.1.1 Aubach spring

ANN model is very good with a KGE' of 0.88 (Table 4). The snow-influenced period from April to mid-June is accurately modelled, as are the peaks in summer and early autumn (Fig. 2a4a). The highest peaks of the whole time series occurring in February, July and November are only slightly underestimated. The model is balanced and accurate on volume ( $\beta=0.93$ ), variability ( $\gamma=1.01$ ) and shape and timing ( $r=0.91$ ). The model is very good for simulating high flows and is decent on low 405 flows, but could be improved especially on shape and timing ( $r_H=0.84$ ,  $r_L=0.66$ ). The slightly higher value of  $\gamma_L$  (1.26) may be related to the tendency of the model to “oscillate” during low/medium flows (e.g. in September, Fig. E1a). This wave-like behaviour may be related to a high sensitivity to precipitation events or to an inappropriate learning from other data. DE is very good (0.14, Fig. 5a7a). The model shows negative dynamic and constant errors with a higher share of high flows, which points a small underestimation of the occurrence of high flows.

410 Reservoir model is decent with a KGE' of ~~0.67~~0.69 (Table 4), but the model fails to accurately reproduce the discharges in all seasons. There is a deficit in water during winter/early spring and an excess during spring (Fig. 2a4a). The model is balanced and accurate on ~~volume ( $\beta=0.94$ ) and~~ variability ( ~~$\gamma=1.05$~~ 0.91), but has middling shape and timing ( ~~$r=0.68$~~ 0.78) ~~and underestimates volume ( $\beta=0.81$ )~~. The model is particularly bad for simulating low flows, with high errors on volume ( ~~$\beta_L=1.25$~~ 1.18), variability ( ~~$\gamma_L=2.01$~~ 1.26) and shape and timing ( ~~$r_L=0.40$~~ 0.41). The simulated high flows are decent, although 415 they ~~are also poor~~can be improved on shape and timing ( ~~$r_H=0.54$~~ 0.68) ~~and volume ( $\beta_H=0.70$ )~~. DE is ~~somewhat insufficient~~good (~~0.45~~0.26, Fig. 5a7a). The model has ~~a positive-negative dynamic and constant errors and a negative constant error~~, with a higher share of ~~low-high~~ flows, ~~which highlight a substantial underestimation of the occurrence of low flows~~. These errors ~~are probably~~can be either due to (i) a miscalibration of the snow routine, retaining too much water as snow in winter and thus releasing too much in warmer periods, (ii) ~~the uncertainties related to the meteorological data in~~ 420 ~~mountainous catchments, or (iii) the snow dynamics which cannot be taken into account within the KarstMod platform, e.g. by adding a snow storage above the epikarst (Chen et al., 2018)~~.

In October, a series of peaks is not well captured by the outputs of both models (Fig. 2a4a). A plausible explanation is that the inputs do not capture the respective local precipitation events due to the location of the climate stations outside the catchment.

425 The modelling of discharges from Aubach spring is challenging due to the large elevation differences and the heterogeneity of precipitation on the catchment. This makes it difficult to provide accurate data to the model, especially with regard to snow dynamics. The reservoir model is particularly confronted with these aspects because (i) it can only handle a single precipitation input (from one weather station or interpolated from several stations) and (ii) the snow dynamics must be simulated by a snow module. As these preprocessings ~~are not included in the model calibration and are mostly performed~~

430 manually cannot really catch the spatial heterogeneity of complex snow processes, they strongly limit the model performance (Çallı et al., 2022). Leaving aside the mismatches related to inadequate meteorological inputs, the structure of the reservoir model seems appropriate to simulate the hydrological response of the spring. In contrast, the ANN model is able to consider snow dynamics without any preprocessing, using only the precipitation and temperature time series during calibration. It shows a great versatility with respect to the input data, similar to that of a two-dimensional approach.

#### 435 4.1.2 Gato Cave spring

ANN model is very good with a KGE' of 0.91 (Table 4), but the model struggles to reproduce the discharges during flood events (Fig. 2b4b). Very high peaks are either overestimated (e.g. May 2012, April 2013, March 2014) or underestimated (e.g. December 2011, November 2012, March 2013). The model is balanced and accurate on volume ( $\beta=0.98$ ), variability ( $\gamma=0.97$ ) and shape and timing ( $r=0.92$ ). The model is good for simulating high flows and is somewhat decent on low flows. 440 It shows a slight lack on shape and timing on both high and low flows ( $r_H=0.82$ ,  $r_L=0.82$ ), and also seems to overestimate low flows ( $\beta_L=1.32$ ). In the same way as Aubach ANN model, the slightly high variability ( $\gamma_L=1.19$ ) may be related to the “oscillations” that can be observed especially on medium and low flows (e.g. January 2012, May 2013, Fig. E1b).

Reservoir model is very good with a KGE' of 0.85 (Table 4), although the model tends to slightly underestimate the discharges during high-flow events ( $\beta_H=0.82$ ; Fig. 2b4b). This seems to happen when precipitation occur during several days 445 without reaching really high values, which may indicate either (i) some kind of hysteresis functioning with flow occurring after a connection has been made in the system, or (ii) inflows into the system that are not taken into account in the model. The model is balanced and accurate on variability ( $\gamma=0.910.92$ ) and shape and timing ( $r=0.950.96$ ), but generally underestimates volume ( $\beta=0.88$ ). The model has good performance on high flows and is decent on low flows. After flood periods, the model seems to simulate a slower draining than observed – higher volume ( $\beta_L=1.221.19$ ) and variability 450 ( $\gamma_L=1.21.27$ ) of low/medium flows – resulting in inaccurate recession periods for which the discharge is overestimated (e.g. November 2011, January 2013, April 2014).

Some periods like November 2012 or February 2015 are not simulated very well by both models (Fig. 2b4b), which may be related to uncertainties in the meteorological data input. DE is decent (0.39) for ANN model and good (0.230.32) for reservoir model (Fig. 5b7b). Both models have a positive dynamic error with a higher share of low flows, which highlight a 455 small underestimation of the occurrence of low flows.

The modelling of discharges from Gato Cave spring shows that both approaches can have great performance given few modelling constraints. Raw precipitation input was used in both models, therefore avoiding additional uncertainties from interpolation or snow preprocessings.

### 4.1.3 Lez spring

460 ANN model is good with a KGE' of 0.7 for discharge (Table 4) and 0.89 for water level (Fig. 35). The high piezometric levels (above 55 m asl) seems a bit too sensitive to precipitation events, especially at the end of 2019 (Fig. 2e4c). On discharges, the model is accurate on variability ( $\gamma=1.13$ ) and shape and timing ( $r=0.93$ ), but underestimates volume ( $\beta=0.74$ ). The overall underestimation of volume mainly comes from high flows ( $\beta_H=0.75$ ) as they are the most represented on the time series. The model is decent on high flows, although having too much variability ( $\gamma_H=1.38$ ). On low flows, the model performs poorly mainly due to high underestimation of volume ( $\beta_L=0.64$ ) and insufficient shape and timing ( $r_L=0.64$ ).  
465 Reservoir model is ~~very~~ good with a KGE' of 0.80.7 for discharge (Table 4) and 0.780.75 for water level (Fig. 35). However, the model fails to reproduce the observed discharge for several months for the period between September 2017-2020 and March 2018-2020 (Fig. 2e4c). During dry periods, there is a too high deficit in the lower reservoirs, leading to a strong delay in the spring response when fresh precipitation occur – the C reservoir having to be replenished beforehand. The model is  
470 balanced and accurate on ~~variability ( $\gamma=1.1$ ) and~~ shape and timing ( $r=0.88$ ), but overestimates variability ( $\gamma=1.15$ ) and underestimates volume ( $\beta=0.880.77$ ). The model is decent on high flows, but has poor variability ( $\gamma_H=1.361.46$ ) and shape and timing ( $r_H=0.670.68$ ), and also ~~slightly~~ underestimates volume ( $\beta_H=0.870.78$ ). On low flows, the model has too much variability ( $\gamma_L=1.261.37$ ) and middling shape and timing ( $r_L=0.76$ ). The piezometric levels are satisfactory when the spring is flowing (greater than 65 m asl), but lose accuracy during dry periods. The model could not reproduce the changes in flow  
475 dynamics at 46 m asl (August 2019, August 2020, Fig. 35). Also, the draining of the aquifer seems to be simulated slower than observed (July 2018, July 2019), which can be a result of the model trying to fit the aforementioned periods during calibration.

On both models, the poor overall KGE' value on low/medium flows is probably due to the small occurrences of low discharges (except 0), thus inducing a high error on volume. DE is good for both ANN (0.31) and reservoir models  
480 (0.290.35) (Fig. 5e7c). Both models have negative dynamic and constant errors with a higher share of high flows, which highlight an underestimation of the occurrence of high flows.

The time series is generally characterised by distinct dry periods without any recharge due to the anthropogenic pumping of water into the saturated zone of the aquifer. These periods are simulated fairly accurately by both models but ANN model is better at simulating first floods after or during dry periods. Several boreholes at the north of the spring showed flow-bearing  
485 structures at 50 m asl (Dausse et al., 2019). These fast water transfer could explain the rapid increases in observed piezometric level and the reactive spring responses. We also suspect an evolution of the carbonate's facies with depth, which could affect the effective porosity of the medium and induce different flow dynamics. These aspects are not considered in the reservoir model which results in poor simulations when the water level is below 60 m asl. However, this failure provides information on the structure of the aquifer, which is valuable for research. On the other hand, ANN model was successful in  
490 learning these particular behaviours, especially as it only had a medium learning time of about 8 years.

#### 4.1.4 Qachqouch spring

ANN model is decent with a KGE' of 0.67 (Table 4), but strongly overestimates low flows at the beginning of December, then underestimates the flood peak at the end of the month (Fig. 2d4d). The model slightly underestimates volume ( $\beta=0.87$ ), and is lacking in variability ( $\gamma=0.75$ ) and shape and timing ( $r=0.82$ ). The high flows are poorly simulated but the low flows are well fitted, although volume is slightly overestimated ( $\beta_L=1.21$ ). The oscillations of the simulated discharges (Fig. E1c) may appear because the model does not account the time needed for the aquifer to replenish and generate an increase of discharge at the spring.

Reservoir model is very good with a KGE' of ~~0.86~~0.83 (Table 4). At the end of the dry period, the low flows are overestimated and the first flood is underestimated (Fig. 2d4d). This may be due to heterogeneous precipitation occurring on highly transmissive parts of the catchment. In this case, the soil available water capacity ( $E_{\min}$ ) – which is necessary for a good simulation of low-flow periods – may not be representative of the whole catchment, thus inducing a more dampened response than observed. The model is balanced and accurate on volume ( $\beta=1.0+1.05$ ) and shape and timing ( $r=0.94+0.93$ ), but slightly lacks in variability ( $\gamma=0.87+0.85$ ). The model is decent on high flows but has middling variability ( $\gamma_H=0.59+0.57$ ) which can be due to the underestimation of the late December flood peak. The low flows and recession periods are slightly overestimated ( $\beta_L=1.1+1.20$  and  $\gamma_L=1.24+1.19$ ).

DE is bad for ANN and reservoir models (0.77 and ~~0.76~~0.84, respectively, Fig. 5d7d). Both models have a positive dynamic error with a higher share of low flows, which highlight an underestimation of the occurrence of low flows. Here, the positive dynamic error is influenced by the constant underestimation of the observed discharge during the dry period (October–December 2019), accounting for more than 50 % of the observations.

The very short data length is particularly detrimental to the ANN model as the learning period is only about ~~3~~4 years. Furthermore, even when data are available, there is a significant amount of time without (relevant) discharge, for which no input-output relation can be learned. Due to the characteristics of the discharge time series, it can be assumed that a much longer time series of daily values would be needed to successfully simulate the discharges of Qachqouch spring. On the other hand, the reservoir model seems more appropriate to simulate Qachqouch spring discharges even with the limited data available. This highlights the strength of conceptual modelling to take into account recharge processes and reservoir replenishment, even on a short dataset with long dry periods.

#### 4.1.5 Unica springs

ANN model is good with a KGE' of 0.73 (Table 4). The model is accurate on volume ( $\beta=1.03$ ) and shape and timing ( $r=0.93$ ), but insufficient on variability ( $\gamma=0.74$ ). The model is good at simulating high flows, although slightly lacking in volume ( $\beta_H=0.87$ ), variability ( $\gamma_H=0.89$ ) and shape and timing ( $r_H=0.79$ ). The model is poor for simulating low flows, which are often significantly overestimated ( $\beta_L=1.92$ ), especially the recession periods which systematically have a slower draining (Fig. 2e4e). The overestimation of low flows could be the result of the model trying to better fit the high-flow periods during

training, which may shift the whole discharge curve slightly towards the upper limits. The model also seems to be too sensitive regarding precipitation events, hence the wave-like behaviour of the simulated time series (Fig. E1d). DE is bad (0.72, Fig. 5e7e). The model has a negative dynamic error and a positive constant error with a higher share of low flows, which highlights an overestimation of the occurrence of low flows.

Reservoir model is good with a KGE' of 0.780.77 (Table 4). The model is balanced and accurate on variability ( $\gamma=0.940.89$ ) and shape and timing ( $r=0.940.93$ ), but has shortcomings on volume ( $\beta=0.80.77$ ). In some winter months (December 2017, March 2018), the model has a delayed response of the rising limb (Fig. 2e4e), which may be due to a slightly wrong parametrisation of the snow routine. The model is good on high flows, but shape and timing ( $r_H=0.820.81$ ) and volume ( $\beta_H=0.750.74$ ) could be improved. The model accurately simulates low flows volume, but has too much variability ( $\gamma_L=1.341.25$ ) and is middling on shape and timing ( $r_L=0.760.78$ ). The difficulty of the model to reproduce the depletion of the capacitive function may be due to the size and complexity of the catchment and the very specific influence of poljes draining over the catchment, which cannot be simulated within the KarstMod platform. DE is very good (0.160.18, Fig. 5e7e). The model has negative dynamic and constant errors with a higher share of high flows, which highlight a small underestimation of the occurrence of low flows.

Both models were unable to reproduce the plateau-like behaviour observed at very high discharges (Fig. 2e4e), which is due to the flooding of a polje at Unica springs that influences the monitoring station (Mayaud et al., 2022). They are simulated as separate peaks, which is false in terms of model accuracy but may also have some underlying conceptual truth. Only two meteorological stations were considered, which is very few for such a large catchment (820 km<sup>2</sup>). Moreover, the major recharge area (Javorniki plateau) does not have any direct climate data available. Both models have difficulties in consistently reproducing the very particular hydrological functioning of the system (influenced by polje and surface water). ANN model is more reactive, which helps for reproducing the dynamics of high floods peaks but hinders the simulation of low flows. Reservoir model has better dynamics for medium and low flows but does not always manage to reproduce high floods peaks, which may be a consequence of the simple structure of the model.

## 4.2 Source of uncertainties

Both ANN and reservoir models have similar trends on water volume and hydrological variability (Fig. 46). Overall volumes are great with  $\beta$  ranging from 0.74 to 1.031.05. High-flow volumes are systematically underestimated with  $\beta_H$  ranging from 0.710.70 to 1.010.98. Low-flow volumes are mainly overestimated –  $\beta_L$  ranging from 0.99 to 1.92 – except for on ANN model on Lez spring with  $\beta_L$  of 0.64 and 0.72. Overall hydrological variability is mainly underestimated, with only Lez and Aubach springs having  $\gamma$  values slightly above 1. High-flow hydrological variability doesn't show a distinct trend, being either overestimated or underestimated depending on the studied system. Low-flow hydrological variability is mainly overestimated with  $\gamma_L$  ranging from 0.95 to 2.011.37. These overestimations may be due to (i) improper – and generally softer – simulation of recession periods or (ii) too high sensitivity to precipitation events, especially in ANN models,

555 inducing discharges oscillations during recession and low-flow periods. The performance on shape and timing ( $r$ ) are mixed between the two approaches. They depend mainly on the system studied and the quality of the model, but also on the hydrological period considered.

These similar results between the two approaches highlight a common struggle to simulate extreme water conditions. As ANN and reservoir modelling approaches are very different, explanation must be sought in common factors to both approaches such as input data, observed data, internal/external system dynamics or the consideration of extreme events during calibration:

- Input data: Generally, in one-dimensional modelling approaches, input data only comes from at most few meteorological stations and does not accurately reflect the heterogeneity of meteorological processes on a catchment. Spatial variability of precipitation can be very high and not fully captured by meteorological stations, (i) 565 resulting in different travel time and generating a different response at the spring (Ollivier et al., 2020), and (ii) hindering the simulation of very high flows (Pereira et al., 2014; Hohmann et al., ~~2020~~2021) – especially in areas where strong convective storms are frequent (Lobligeois et al., 2014). McMillan et al. (2018) suggested that uncertainties in precipitation data are about 0–10 % at point scale but can go up to 40 % when considering interpolation uncertainties. Temperature data are generally less heterogeneous than precipitation, although it can be affected by complex topography (Aalto et al., 2017). In the case of snow-covered areas, it can result in strong uncertainties on the timing of snow accumulation and melting (Zhang et al., 2016), and therefore the recharge of the aquifer. The uncertainties related to precipitation and temperature input in one-dimensional hydrological models can thus – partly – explain the difficulties to reproduce extreme events (Lobligeois et al., 2014; Huang et al., 2019; Ollivier et al., 2020; Bittner et al., 2021), especially high flows.
- Observed data: Discharge time series are generally derived from water height measured at the spring, using water level–discharge calibration curves. Numerous uncertainties are related to this determination method (Pelletier, 1988), including extrapolation errors for extreme values (Di Baldassarre and Montanari, 2009; Moges et al., 2021). Extreme events occur more rarely and are harder to measure, especially high flows. This can result in inaccurately observed discharge time series that are difficult to reproduce with simulations (e.g. Unica springs at very high 580 flows). The uncertainties related to discharge measurements are highly dependent on the quality of the gauging station and usually range between 10–40 % (McMillan et al., 2018). Although they are expected to be higher in a karst context (Westerberg et al., 2016), some authors reported uncertainties of about 20 % (Jeannin et al., 2021) or 10–15 % (Katz et al., 2009).
- Internal/external system dynamics: Karst systems are inherently complex media. Internal dynamics are not necessarily captured in hydrological models (Sidle, 2006, 2021; Hartmann et al., 2017) and can be related to numerous processes in karst media, e.g. the saturation state of the system, surface water exchanges, temporary storage of water, incoming or outgoing flows from/to another aquifer, change of physical properties beyond a certain level, or karst features such as poljes or sinkholes. These complex processes do not occur systematically and 585

can change from year to year (Ollivier et al., 2020). This can lead to difficulties in training ANN models or in  
590 adapting the structure of reservoir models.

- Extreme events during calibration: ANN and reservoir models are both trained on a calibration period. By definition, extreme events are rare. Therefore, models may have less opportunities to successfully fit model parameters to such events (Seibert, 2003), preferring more balanced parameters that are appropriate to the rest – and most – of the time series (Onyutha, 2019). In addition, models are generally calibrated over the whole time series  
595 using one performance criterion against observed data. In this case, extreme events are not explicitly emphasised in the objective function. A solution could be to give more weight to the reproduction of certain parts of the time series, such as flood and dry periods (Singh and Bárdossy, 2012), or to use different model optimisation techniques, such as cross-validation (Wilks, 2011).

Both approaches can also benefit from a careful assessment of the calibration period. For example, the ANN model is  
600 thought to overestimate low flows in Unica springs by trying to fit the plateaus at very high discharges. In Lez spring, the reservoir model simulates a slower draining in the aquifer (piezometric level) because it does not account for a potential change in underground dynamics. These limitations emphasise the need for a meticulous investigation of the results in regard to the characteristics of the system and the input data. Such errors can be avoided or lessened by excluding abnormal periods during the calibration, which can be justified by inaccurate input data or limitation in the conceptual model.

### 605 4.3 Comparison of general model properties

The main findings of this study are presented in Table 5. The extensive analysis of high and low flows did not show a clear trend, but did reveal slight differences between the two approaches for this study. For high-flow periods, results slightly favour the ANN approach (except for Qachqouch spring), with consistently accurate volumes and shape and timing (Fig. 46). ANN models also tend to achieve higher flows than reservoir models (Fig. 24); due to the noticeable/strong karstification of the studied systems, the high occurrence of high discharge data may benefit the learning of the ANN models. On the other hand, reservoir models are more dependent on the relevance and the quality of the input data preprocessing, thus can be more affected by the uncertainties presented in Sect. 4.2, especially regarding high flows. For low-flow periods, results slightly favour the reservoir approach (except for Aubach spring), with ~~very~~ good estimation of volumes and only a slight overestimation of the hydrological variability (Fig. 46). The conceptual representation of the aquifer with reservoirs and transfer functions may help to simulate the recharge process (especially for inertial systems): a precipitation event will not directly result in a discharge increase at the spring if the reservoir is not fully saturated. On the other hand, ANN models seem to not always account for the time needed for the aquifer to replenish, inducing wave-like behaviours during medium- and low-flow periods (Fig. E1), which can hinder the simulation of low flows. The water level (Lez spring) was correctly simulated by both approaches, with only some imprecision during dry periods (Fig. 35).

**Table 5: Advantages and drawbacks of ANN and reservoir models, based on the results of this research.**

	ANN models	Reservoir models
Advantages	<ul style="list-style-type: none"> <li>- Fast and reliable</li> <li>- Flexible regarding input data</li> <li>- Slightly better on high flows</li> <li>- Can be used to gain knowledge about input data, catchment delineation, recharge processes</li> </ul>	<ul style="list-style-type: none"> <li>- The simulation is supported by a conceptual model</li> <li>- Slightly better on low flows</li> <li>- Can be used to gain knowledge about system functioning</li> <li>- Can work with short observed time series</li> </ul>
Drawbacks	<ul style="list-style-type: none"> <li>- Struggle to reproduce extreme events</li> <li>- Need medium/long observed time series for a proper learning</li> <li>- Essentially a black-box approach</li> </ul>	<ul style="list-style-type: none"> <li>- Struggle to reproduce extreme events</li> <li>- Input data generally need preprocessing</li> <li>- Can be time consuming</li> <li>- Potential platform/coding limitations</li> </ul>

ANN models are flexible and provide numerous advantages over reservoir models with respect to input data. It can easily integrate meteorological processes (e.g. snow dynamics, evapotranspiration) without any preprocessing of the raw data, whereas it is generally calculated beforehand in reservoir models. It is also possible to add a large amount of raw data in ANN models and let the model select those relevant for a good simulation, which make the modelling easier and also can give insight into the input data or catchment characteristics (Wunsch et al., 2022). This helps to avoid additional uncertainties related to (i) arbitrary decisions over the raw data (e.g. choosing precipitation from one station rather than another), (ii) interpolation (when data from several meteorological stations over a catchment are available) or (iii) preprocessing (e.g. snow routine, potential evapotranspiration). This great flexibility regarding input data makes ANN model close to a 2D or semi-distributed approach. If necessary, the transition between 1D and 2D input data are comparably easy, whereas in reservoir models this usually involves changing or adapting the tool.

Reservoir models do not need long calibration period to provide accurate and relevant simulation results. In contrast, a very short time series or a short time series with long dry periods can be detrimental for the learning of ANN model, which seems to benefit from long calibration periods of relevant discharge (at least 5 years). We have seen that the ANN model has difficulties in simulating the flows of the Qachqouch spring, mainly because of (i) the short calibration period, and (ii) the long low water periods which are not relevant for training the model. On the other hand, the reservoir model has been able to integrate key elements (e.g. double porosity, matrix-conduit exchanges, fast conduit transfer in wet periods) by relying on the conceptual model.

The ANN approach does not require any prior knowledge of the system and inherently considers model structure and parameters. This makes the modelling process easier and faster thus saving the operator a great amount of time. On the other

hand, reservoir models require a significant investment in reading the literature, analysing expert knowledge, and doing trial and error during model design. Moreover, the cost of a change of structure is not trivial. Depending on the modelling platform (e.g. software, raw code), it may take more or less time – or even be impossible – to take certain elements into account. For example, in this study, the KarstMod platform does not allow (i) different porosities to be considered in the same reservoir, leading to difficulties in modelling the piezometric levels during dry periods for the Lez system; (ii) using different  $E_{min}$  values, which may benefit the Qachqouch model; ~~or~~ (iii) considering polje and surface water influence in the Unica model; or (iv) considering snow dynamics in the structure of the Aubach model.

Both ANN and reservoir models can be used for research purpose. Model structure, transfer functions and parameters are explicitly expressed in reservoir models, which can provide valuable insights into the hydrogeological structure of the reservoir and the internal processes of the karst system, e.g. (i) the relative contributions of fast and slow flows; (ii) the draining of each compartment; (iii) the activation thresholds of the overflow transfer functions (either to the spring or out of the system); (iv) the changes in flow dynamics with respect to dry and wet periods; and (v) the exchanges between the matrix and conduit compartments. In comparison, ANN models act rather as a “black-box”, whose parameters are more difficult to exploit and associate with the hydrological functioning of a system. However, ANN model can help to explore input data, thus indirectly providing insights into catchment delineation or external recharge processes (Wunsch et al., 2022).

## 5 Conclusion

Our objective was to provide researchers and stakeholders with guidelines for choosing either artificial neural networks or reservoir models to simulate karst spring discharges, depending on their purpose, data availability, data length and time budget. Five test sites were considered, allowing different hydrological conditions and input data to be studied. The results of ANN and reservoir models were compared on the basis of several performance criteria, distinguishing between high- and low-flow conditions. Both models succeeded in simulating spring discharges satisfactorily, although struggling to reproduce extreme events (drought, flood), generally overestimating low flows and underestimating high flows. This can be related to common problems in hydrological modelling regarding uncertainties in the input data or observed data, internal/external system dynamics or the consideration of extreme events during calibration.

ANN models seem robust for reproducing high-flow conditions and reservoir models for reproducing low-flow conditions. The input data are also a critical factor of choice. Reservoir models can work with relatively short time series while ANN models need a minimum number of relevant years to learn the functioning of a karst system. On the other hand, ANN models are very flexible on the format and amount of input data. It can learn many meteorological processes with no prior need for preprocessing the raw data, as well as use several time series for a single variable. This avoids arbitrary interpolation decisions (e.g. precipitation between several stations), parameter definitions (e.g. snow routine) or meteorological calculation (e.g. potential evapotranspiration), and allows these aspects to be integrated into the model calibration.

Both ANN and reservoir models can be used for karst aquifer management, flood forecasting and system characterisation.

675 ANN models may be more appropriate for simulating high flows, delineating catchments, or assessing external recharge processes. Reservoir models seems more robust for simulating low flows and gaining insights into the internal functioning of a system. ANN models can also be interesting time-wise as (i) they do not require any prior knowledge of the system and (ii) model design is more flexible regarding input data and system functioning. ~~Given appropriate input data, both models are suited for climate change predictions, as they showed accurate simulations with long calibration periods. However, the operator should keep in mind that the models (i) have difficulty in reproducing extreme events, which are likely to occur more frequently, and (ii) can only reproduce what they know or have learned during the calibration period and cannot take into account the impact of the evolution of recharge processes on the aquifer functioning.~~

685 One of the difficulties this paper faced was to distinguish the general limitations of the reservoir modelling approach from those specific to the chosen modelling platform. In comparison to user-defined models, the modelling platform constrains the structure and the transfer functions of the conceptual model. Remaining within the KarstMod platform provided the time advantages of a turnkey toolbox (which are widely used in research and by stakeholder), but limited the possibilities of the conceptual models. ~~For example, model performance could have been improved by considering the evolution of system properties with depth, or snow accumulation and melting could have been more accurate by including its parameters in the model calibration. Implementation of a meteorological module in KarstMod for directly calibrating the parameters of the snow routine is besides under implementation.~~

690

**Appendix A: Location of the study sites**

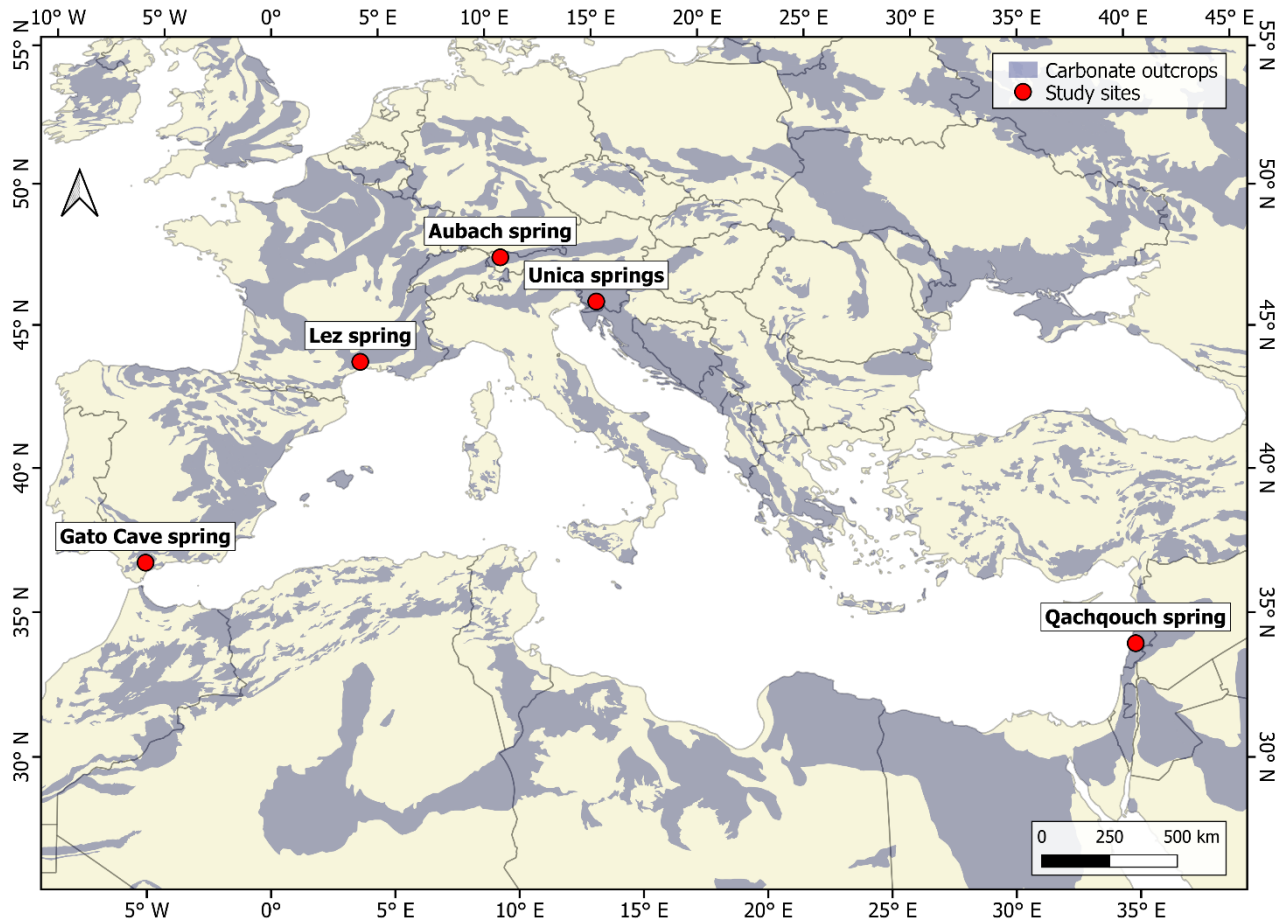


**Figure A1: Location of the study sites (carbonate outcrops from Chen et al. (2017)).**

## Appendix BA: Origin of the meteorological data

**Table BA.1:** Origin of the meteorological data (i) P, (ii) T, (iii) R<sub>so</sub>, (iv) RH, (v) U, (vi) AET, (vii) R<sub>s</sub>, (viii) S and (ix) NS refer to (i) Precipitation, (ii) Temperature, (iii) Clear-sky solar radiation, (iv) Relative humidity, (v) Wind speed, (vi) Actual evapotranspiration, (vii) Solar radiation, (viii) Snow and (ix) New snow, respectively.

Spring	Station	Altitude [m]	Latitude [°]	Longitude [°]	Data measured
	Diedamskopf	1790	47.3389	10.0256	P, T, R <sub>so</sub>
Aubach	Oberstdorf	806	47.3984	10.2759	P, T, R <sub>so</sub>
	Walmendinger Horn	1650	47.3219	10.1225	P, T, R <sub>so</sub>
Gato Cave	Grazalema	901	36.7678	-5.3658	P, T
	Prades-le-Lez	69	43.7176	3.8573	P, T, RH, U
	Puéchabon	250	43.7414	3.5958	AET
Lez	Saint-Martin-de-Londres	214	43.7903	3.7326	P
	Sauteyrargues	150	43.8345	3.9207	P
	Valflaunès	155	43.8001	3.8707	P
	<i>950 m station</i>	950	33.9180	35.6763	P, T, RH, U, R <sub>s</sub>
Qachqouch	<i>1700 m station</i>	1700	34.0253	35.8360	P, T, RH, U, R <sub>s</sub>
	Cerknica	569	45.7956	14.3634	P, S, NS
Unica	Postojna	533	45.7661	14.1932	P, T, RH, S, NS

## 700 Appendix CB: Calculation details for the Thiessen's polygons interpolation method

The Thiessen's polygons interpolation method consists of calculating a weighted average of precipitation data from several meteorological stations. The contribution percentages of the stations are proportional to their influence area on the catchment. An influence area corresponds to a polygon where the precipitation is considered to be identical to that measured at the associated meteorological station. The polygons are defined in two steps: (i) drawing the straight-line segments between all adjacent stations and (ii) adding the perpendicular bisectors of each segment, which correspond to the edges of the polygons. The weighted average of the precipitation  $P_{TH}$  is calculated with the following equation:

$$P_{TH} = \frac{\sum_{i=1}^n A_i P_i}{A} \quad (C1)$$

With  $A$  the area of the catchment,  $n$  the number of meteorological stations,  $A_i$  the area of the polygon associated to the  $i^{th}$  station and  $P_i$  the precipitation measured at the  $i^{th}$  station.

### Appendix DC: Calculation details for the snow routine

Accounting for snow accumulation and melting in hydrological modelling can greatly improve model results, especially for regions with high snow volumes. Chen et al. (2018) successfully simulated spring discharge of a mountainous karst system strongly influenced by snow accumulation and melting. They applied a modified version of the HBV snow routine Bergström (1992) proposed by Hock (1999). We used this snow routine as an external KarstMod module (i.e. without internal calibration).

The snow routine simulates snow accumulation and melting over different sub-catchments defined according to altitude ranges. The input data consist in three time series (temperature, precipitation and potential clear-sky solar radiation) and five parameters (temperature threshold, melt coefficient, refreezing coefficient, radiation coefficient and water holding capacity of snow). The potential clear sky solar radiation time series and radiation coefficient are only used when working at an hourly time scale to simulate a more refined snowmelt by considering sun exposure. The parameters values were estimated by model calibration. We calibrated the temperature threshold, the melt coefficient and the radiation coefficient manually.

Precipitation is considered as snow when the air temperature is below the temperature threshold. Snowmelt begins when the temperature is above the threshold according to a degree-day expression, where snowmelt is a function of the melt coefficient, solar radiation and degrees above the threshold. Runoff starts when the liquid water holding capacity of snow is exceeded. The refreezing coefficient allows to consider the refreezing processes of liquid water in the snow if snowmelt is interrupted (Bergström, 1992). The output of the snow routine is a time series of redistributed precipitation.

### Appendix D: Calibration scores of the reservoir models

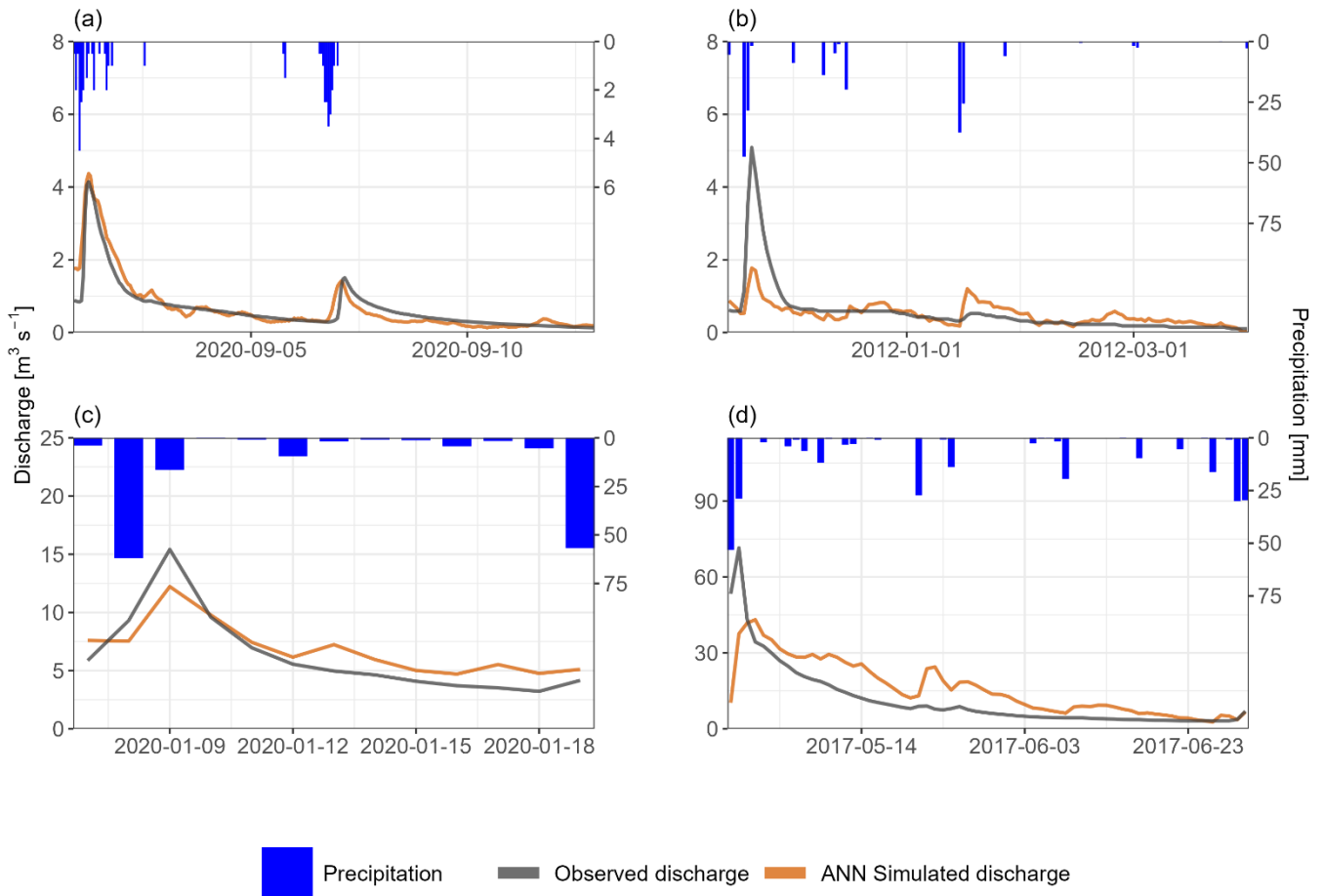
Table D1: Scores of both modelling approaches over the calibration and validation periods with MSE. No results are available on the calibration period for the ANN models, as it corresponds to the learning period of the models. Each component of the composite objective function MSE(O, Z) of the Lez spring has been normalised.

Spring	Calibration period		Validation period	
	ANN	Reservoir	ANN	Reservoir
Aubach	/	0.40	0.26	0.63
Gato Cave	/	1.53	1.53	1.07

<u>Spring</u>	<u>Calibration period</u>		<u>Validation period</u>	
	<u>ANN</u>	<u>Reservoir</u>	<u>ANN</u>	<u>Reservoir</u>
<u>Lez</u>	<u>/</u>	<u>8.63</u>	<u>4.53</u>	<u>8.84</u>
<u>Qachqouch</u>	<u>/</u>	<u>1.17</u>	<u>7.78</u>	<u>2.87</u>
<u>Unica</u>	<u>/</u>	<u>81.57</u>	<u>123.51</u>	<u>152.92</u>

### 735 Appendix E: Examples of wave-like behaviour produced by the ANN model

The periods were selected in such a way that the influence of snow precipitation and melt is zero or almost zero. Precipitation input correspond to either direct observations from a meteorological station, or preprocessed observations with Thiessen's polygon interpolation (Appendix [EB](#)) if there are several meteorological stations.



740 **Figure E1: Examples of wave-like behaviour produced by the ANN model on (a) Aubach, (b) Gato Cave, (c) Qachqouch and (d) Unica springs.**

## Code and data availability

We provide complete codes for ANN models and *.properties* files for reservoir models on Github (Cinkus and Wunsch, 745 2022). Due to redistribution restrictions from several parties, a dataset cannot be provided. However, the data are available from the local authorities upon request. Aubach spring discharge time series and meteorological data from Diedamskopf and Walmendinger Horn stations are available from the office of the federal state of Vorarlberg – division of water management. Meteorological data from Oberstdorf station are available on the DWD Open Data Server (DWD, 2022). Gato Cave spring discharge time series is available from the Confederación Hidrográfica de las Cuencas Mediterráneas Andaluzas (Cuenca 750 Mediterránea Andaluza, 2022) and meteorological data is available in “Datos a la carta” section in Consejería de Agricultura, Pesa, Agua y Desarrollo rural (Consejería de Agricultura, Pesa, Agua y Desarrollo rural, 2022). Lez spring discharge time series is available on the OSU OREME website (SNO KARST, 2019), water level time series can be requested from Montpellier Méditerranée Métropole, and meteorological data are available on request from Météo-France. Qachqouch discharge time series and meteorological data are available on request from the Department of Geology at the American 755 University of Beirut. Unica spring discharge time series and meteorological data are available from ARSO (Slovenian Environment Agency) (ARSO, 2021a, b).

## Author contribution

GC, AW, NM, TL, HJ and NG conceptualised the study and designed the methodology. GC and AW developed the software code. GC and AW performed the experiments and investigated and visualised the results. GC and ZC performed formal 760 analysis. GC wrote the original paper draft with contributions from AW, NR, JD, JFO. All authors contributed to the interpretation of the results and review and editing of the paper draft. NM and HJ supervised the work.

## Competing interests

The authors declare that they have no conflict of interest.

## Acknowledgements

765 We thank the French Ministry of Higher Education and Research for the thesis scholarship of G. Cinkus as well as the European Commission for its support through the Partnership for Research and Innovation in the Mediterranean Area (PRIMA) program under Horizon 2020 (KARMA project, grant agreement number 01DH19022A). The data collection and instrumentation on the Qachqouch catchment were funded by USAID and National Academy of Science (Peer Science; project award: 102881; Cycle 3) and KARMA project (L-CNRS in the framework of the PRIMA program; Award# 103895; 770 Project# 25713). Moreover, Beirut and Mount Lebanon Water Establishment are thanked to facilitate the installation of

instruments and access to field sites. We thank the Slovenian Research Agency for financial support within the project “Infiltration processes in forested karst aquifers under changing environment” (No. J2-1743) and the Karst Research Programme (No. P6-0119). We further thank the National Agency of Research of the Spanish Ministry of Science, Innovation and Universities for the funding of the KARMA project (PCI2019-103675) and the Autonomous Government of Andalusia (Spain) for the funding of the Research Group RNM-308. For the data provided, we also acknowledge the French Karst National Observatory Service (SNO KARST, 2019), the French national meteorological service Météo-France, the office of the federal state of Vorarlberg – division of water management, the German Meteorological Service, the Slovenian Environment Agency (ARSO, 2021a, b) and the Meteorological National Agency (AEMET).

The manuscript was written with the Rmarkdown framework (Allaire et al., 2021; Xie et al., 2018, 2020), using R (R Core Team, 2021) and the following packages: readxl, readr, dplyr, tidyr, ggplot2, lubridate (Wickham et al., 2019), cowplot (Wilke, 2020), flextable (Gohel, 2021), hydroGOF (Mauricio Zambrano-Bigiarini, 2020) and padr (Thoen, 2021). We programmed our ANN models in Python 3.8 (van Rossum, 1995), using the following frameworks and libraries: Numpy (van der Walt et al., 2011), Pandas (McKinney, 2010; Reback et al., 2021), Scikit-Learn (Pedregosa et al., 2018), Matplotlib (Hunter, 2007), Bayesian Optimization (Nogueira, 2014), TensorFlow 2.7 (Abadi et al., 2016) and its Keras API (Chollet et al., 2015).

## References

- Aalto, J., Riihimäki, H., Meineri, E., Hylander, K., and Luoto, M.: Revealing topoclimatic heterogeneity using meteorological station data, *Intern. J. Climatol.*, 37, 544–556, <https://doi.org/10.1002/joc.5020>, 2017.
- Abadi, M., Agarwal, A., Barham, P., Brevdo, E., Chen, Z., Citro, C., Corrado, G. S., Davis, A., Dean, J., Devin, M., Ghemawat, S., Goodfellow, I., Harp, A., Irving, G., Isard, M., Jia, Y., Jozefowicz, R., Kaiser, L., Kudlur, M., Levenberg, J., Mane, D., Monga, R., Moore, S., Murray, D., Olah, C., Schuster, M., Shlens, J., Steiner, B., Sutskever, I., Talwar, K., Tucker, P., Vanhoucke, V., Vasudevan, V., Viegas, F., Vinyals, O., Warden, P., Wattenberg, M., Wicke, M., Yu, Y., and Zheng, X.: TensorFlow: Large-Scale Machine Learning on Heterogeneous Distributed Systems, arXiv:1603.04467 [cs], 2016.
- 795 Addor, N. and Melsen, L. A.: Legacy, Rather Than Adequacy, Drives the Selection of Hydrological Models, *Water Resources Research*, 55, 378–390, <https://doi.org/10.1029/2018WR022958>, 2019.
- Allaire, J., Xie, Y., McPherson, J., Luraschi, J., Ushey, K., Atkins, A., Wickham, H., Cheng, J., Chang, W., and Iannone, R.: Rmarkdown: Dynamic documents for r. <https://cran.r-project.org/package=rmarkdown>, 2021. Last access: 12 October 2022.
- Allen, R. G., Pereira, L. S., Raes, D., Smith, M., and FAO (Eds.): Crop evapotranspiration: Guidelines for computing crop water requirements, Food and Agriculture Organization of the United Nations, Rome, 1998.
- 800 Andreo, B., Vadillo, I., Carrasco, F., Neukum, C., Jiménez, P., Goldscheider, N., Hötzl, H., Vías, J., Pérez, I., and Göppert, N.: Precisiones sobre el funcionamiento hidrodinámico y la vulnerabilidad a la contaminación del acuífero kárstico de la

- sierra de líbar (provincias de Málaga y Cádiz, sur de España) a partir de un ensayo de trazadores., *Rev. Soc. Geol. Esp.*, 17, 187–198, 2004.
- 805 Andreo, B., Goldscheider, N., Vadillo, I., Vías, J., Neukum, C., Sinreich, M., Gavilán, P., Brechenmacher, J., Carrasco, F., Hötzl, H., Perles, M., and Zwahlen, F.: Karst groundwater protection: First application of a Pan-European Approach to vulnerability, hazard and risk mapping in the Sierra de Lívar (Southern Spain), *Sci. Total Environ.*, 357, 54–73, <https://doi.org/10.1016/j.scitotenv.2005.05.019>, 2006.
- ARSO: Ministry of the Environment and Spatial Planning, Slovenian Environment Agency, Archive of hydrological data.
- 810 Available online: <http://vode.arso.gov.si/hidarhiv/>, 2021a. Last access: 12 October 2022.
- ARSO: Ministry of the Environment and Spatial Planning, Slovenian Environment Agency, Archive of meteorological data. Available online: <http://www.meteo.si/>, 2021b. Last access: 12 October 2022.
- Bakalowicz, M.: Karst groundwater: A challenge for new resources, *Hydrogeol. J.*, 13, 148–160, <https://doi.org/10.1007/s10040-004-0402-9>, 2005.
- 815 Bergström, S.: THE DEVELOPMENT OF A SNOW ROUTINE FOR THE HBV-2 MODEL, *Hydrol. Res.*, 6, 73–92, <https://doi.org/10.2166/nh.1975.0006>, 1975.
- Bergström, S.: The HBV model - its structure and applications, *SMHI*, 4, 32, 1992.
- Bittner, D., Parente, M. T., Mattis, S., Wohlmuth, B., and Chiogna, G.: Identifying relevant hydrological and catchment properties in active subspaces: An inference study of a lumped karst aquifer model, *Adv. Water. Resour.*, 135, 103472, <https://doi.org/10.1016/j.advwatres.2019.103472>, 2020.
- 820 Bittner, D., Richieri, B., and Chiogna, G.: Unraveling the time-dependent relevance of input model uncertainties for a lumped hydrologic model of a pre-alpine karst system, *Hydrogeol. J.*, 29, 2363–2379, <https://doi.org/10.1007/s10040-021-02377-1>, 2021.
- [Çalli, S. S., Çalli, K. Ö., Tuğrul Yılmaz, M., and Çelik, M.: Contribution of the satellite-data driven snow routine to a karst hydrological model, \*Journal of Hydrology\*, 607, 127511, <https://doi.org/10.1016/j.jhydrol.2022.127511>, 2022.](#)
- 825 Chen, Z. and Goldscheider, N.: Modeling spatially and temporally varied hydraulic behavior of a folded karst system with dominant conduit drainage at catchment scale, Hochifien, Alps, *J. Hydrol.*, 514, 41–52, 2014.
- Chen, Z., Auler, A. S., Bakalowicz, M., Drew, D., Griger, F., Hartmann, J., Jiang, G., Moosdorf, N., Richts, A., Stevanovic, Z., Veni, G., and Goldscheider, N.: The World Karst Aquifer Mapping project: Concept, mapping procedure and map of Europe, *Hydrogeol J.*, 25, 771–785, <https://doi.org/10.1007/s10040-016-1519-3>, 2017.
- 830 Chen, Z., Hartmann, A., Wagener, T., and Goldscheider, N.: Dynamics of water fluxes and storages in an Alpine karst catchment under current and potential future climate conditions, *Hydrol. Earth Syst. Sci.*, 22, 3807–3823, <https://doi.org/10.5194/hess-22-3807-2018>, 2018.
- Cheng, S., Qiao, X., Shi, Y., and Wang, D.: Comparison of Machine Learning Methods for Predicting Karst Spring Discharge in North China, *arXiv:2007.12951 [physics]*, 2020.
- 835 Chollet, F. et al.: Keras, <https://github.com/keras-team/keras>, 2015. Last access: 12 October 2022.

- Cinkus, G. and Wunsch, A.: busemorose/ANN-Reservoir\_model-code: Model code release, Zenodo [code], <https://doi.org/10.5281/zenodo.7242077>, 2022.
- Conradt, T., Wechsung, F., and Bronstert, A.: Three perceptions of the evapotranspiration landscape: Comparing spatial patterns from a distributed hydrological model, remotely sensed surface temperatures, and sub-basin water balances, *Hydrol. Earth Syst. Sci.*, 17, 2947–2966, <https://doi.org/10.5194/hess-17-2947-2013>, 2013.
- Consejería de Agricultura, Pesa, Agua y Desarrollo rural: <http://www.redhidrosurmedioambiente.es/saih/presentacion>, last access: 12 October 2022.
- Cuenca Mediterránea Andaluza: <https://hispagua.cedex.es/instituciones/confederaciones/andalucia>, last access: 12 October 2022.
- Dausse, A., Leonardi, V., and Jourde, H.: Hydraulic characterization and identification of flow-bearing structures based on multi-scale investigations applied to the Lez karst aquifer, *J. Hydrol. Reg. Stud.*, 26, 100627, <https://doi.org/10.1016/j.ejrh.2019.100627>, 2019.
- Di Baldassarre, G. and Montanari, A.: Uncertainty in river discharge observations: A quantitative analysis, *Hydrol. Earth Syst. Sci.*, 13, 913–921, <https://doi.org/10.5194/hess-13-913-2009>, 2009.
- Doummar, J. and Aoun, M.: Occurrence of selected domestic and hospital emerging micropollutants on a rural surface water basin linked to a groundwater karst catchment, *Environ. Earth Sci.*, 77, 351, <https://doi.org/10.1007/s12665-018-7536-x>, 2018.
- Doummar, J., Hassan Kassem, A., and Gurdak, J. J.: Impact of historic and future climate on spring recharge and discharge based on an integrated numerical modelling approach: Application on a snow-governed semi-arid karst catchment area, *J. Hydrol.*, 565, 636–649, <https://doi.org/10.1016/j.jhydrol.2018.08.062>, 2018.
- Dubois, E.: Analysis of high resolution spring hydrographs and climatic data: Application on the Qachqouch spring (Lebanon), PhD thesis, American University of Beirut, 2017.
- Dubois, E., Doummar, J., Pistre, S., and Larocque, M.: Calibration of a lumped karst system model and application to the Qachqouch karst spring (Lebanon) under climate change conditions, *Hydrol. Earth Syst. Sci.*, 24, 4275–4290, <https://doi.org/10.5194/hess-24-4275-2020>, 2020.
- DWD: <https://opendata.dwd.de/>, last access: 12 October 2022.
- Fleury, P., Plagnes, V., and Bakalowicz, M.: Modelling of the functioning of karst aquifers with a reservoir model: Application to Fontaine de Vaucluse (South of France), *J. Hydrol.*, 345, 38–49, <https://doi.org/10.1016/j.jhydrol.2007.07.014>, 2007.
- Fleury, P., Ladouche, B., Conroux, Y., Jourde, H., and Dörfliger, N.: Modelling the hydrologic functions of a karst aquifer under active water management The Lez spring, *J. Hydrol.*, 365, 235–243, <https://doi.org/10.1016/j.jhydrol.2008.11.037>, 2009.
- Ford, D. and Williams, P.: Karst Hydrogeology, in: *Karst Hydrogeology and Geomorphology*, John Wiley & Sons, Ltd, 103–144, <https://doi.org/10.1002/9781118684986.ch5>, 2007.

- Gabrovšek, F., Kogovšek, J., Kovačič, G., Petrič, M., Ravbar, N., and Turk, J.: Recent Results of Tracer Tests in the Catchment of the Unica River (SW Slovenia), *Acta Carsologica*, 39, <https://doi.org/10.3986/ac.v39i1.110>, 2010.
- Gohel, D.: *Flextable: Functions for tabular reporting*, Manual, 2021.
- 875 Goldscheider, N.: Fold structure and underground drainage pattern in the alpine karst system Hochiften-Gottesacker, *Eclogae Geol. Helv.*, 98, 1–17, <https://doi.org/10.1007/s00015-005-1143-z>, 2005.
- Goldscheider, N.: Overview of Methods Applied in Karst Hydrogeology, in: *Karst Aquifers and Engineering*, edited by: Stevanović, Z., Springer International Publishing, Cham, 127–145, [https://doi.org/10.1007/978-3-319-12850-4\\_4](https://doi.org/10.1007/978-3-319-12850-4_4), 2015.
- [Goldscheider, N., Chen, Z., Auler, A. S., Bakalowicz, M., Broda, S., Drew, D., Hartmann, J., Jiang, G., Moosdorf, N., Stevanovic, Z., and Veni, G.: Global distribution of carbonate rocks and karst water resources, \*Hydrogeol J.\*, 28, 1661–1677, <https://doi.org/10.1007/s10040-020-02139-5>, 2020.](https://doi.org/10.1007/s10040-020-02139-5)
- 880 Gondwe, B. R. N., Merediz-Alonso, G., and Bauer-Gottwein, P.: The influence of conceptual model uncertainty on management decisions for a groundwater-dependent ecosystem in karst, *J. Hydrol.*, 400, 24–40, <https://doi.org/10.1016/j.jhydrol.2011.01.023>, 2011.
- Gupta, H. V., Kling, H., Yilmaz, K. K., and Martinez, G. F.: Decomposition of the mean squared error and NSE performance criteria: Implications for improving hydrological modelling, *J. Hydrol.*, 377, 80–91, <https://doi.org/10.1016/j.jhydrol.2009.08.003>, 2009.
- 885 Hargreaves, G. H. and Samani, Z. A.: Reference Crop Evapotranspiration from Temperature, *Appl. Eng. Agric.*, 1, 96–99, <https://doi.org/10.13031/2013.26773>, 1985.
- Hartmann, A., Lange, J., Aguado, A. V., Mizyed, N., Smiatek, G., and Kunstmann, H.: A multi-model approach for improved simulations of future water availability at a large Eastern Mediterranean karst spring, *J. Hydrol.*, 9, 2012.
- 890 Hartmann, A., Goldscheider, N., Wagener, T., Lange, J., and Weiler, M.: Karst water resources in a changing world: Review of hydrological modeling approaches, *Rev. Geophys.*, 52, 218–242, <https://doi.org/10.1002/2013RG000443>, 2014.
- Hartmann, A., Gleeson, T., Wada, Y., and Wagener, T.: Enhanced groundwater recharge rates and altered recharge sensitivity to climate variability through subsurface heterogeneity, *Proc. Natl. Acad. Sci.*, 114, 2842–2847, <https://doi.org/10.1073/pnas.1614941114>, 2017.
- 895 Hock, R.: A distributed temperature-index ice- and snowmelt model including potential direct solar radiation, *J. Glaciol.*, 45, 101–111, <https://doi.org/10.3189/S0022143000003087>, 1999.
- [Hohmann, C., Kirchengast, G., O, S., Rieger, W., and Foelsche, U.: Small Catchment Runoff Sensitivity to Station Density and Spatial Interpolation: Hydrological Modeling of Heavy Rainfall Using a Dense Rain Gauge Network, \*Water\*, 13, 1381, <https://doi.org/10.3390/w13101381>, 2021.](https://doi.org/10.3390/w13101381)
- 900 ~~[Hohmann, C., Kirchengast, G., O, S., Rieger, W., and Foelsche, U.: Runoff sensitivity to spatial rainfall variability: A hydrological modeling study with dense rain gauge observations, \*Hydrol. Earth Syst. Sci.\*, 1–28, <https://doi.org/10.5194/hess-2020-453>, 2020.](https://doi.org/10.5194/hess-2020-453)~~

- Hu, C., Hao, Y., Yeh, T.-C. J., Pang, B., and Wu, Z.: Simulation of spring flows from a karst aquifer with an artificial neural network, *Hydrol. Process.*, 22, 596–604, <https://doi.org/10.1002/hyp.6625>, 2008.
- Huang, Y., Bárdossy, A., and Zhang, K.: Sensitivity of hydrological models to temporal and spatial resolutions of rainfall data, *Hydrol. Earth Syst. Sci.*, 23, 2647–2663, <https://doi.org/10.5194/hess-23-2647-2019>, 2019.
- Hunter, J. D.: Matplotlib: A 2D Graphics Environment, *Comput. Sci. Eng.*, 9, 90–95, <https://doi.org/10.1109/MCSE.2007.55>, 2007.
- 910 Ioffe, S. and Szegedy, C.: Batch Normalization: Accelerating Deep Network Training by Reducing Internal Covariate Shift, *arXiv:1502.03167 [cs]*, 2015.
- Jeannin, P.-Y., Artigue, G., Butscher, C., Chang, Y., Charlier, J.-B., Duran, L., Gill, L., Hartmann, A., Johannet, A., Jourde, H., Kavousi, A., Liesch, T., Liu, Y., Lüthi, M., Malard, A., Mazzilli, N., Pardo-Igúzquiza, E., Thiéry, D., Reimann, T., Schuler, P., Wöhling, T., and Wunsch, A.: Karst modelling challenge 1: Results of hydrological modelling, *J. Hydrol.*, 600, 126508, <https://doi.org/10.1016/j.jhydrol.2021.126508>, 2021.
- Jukić, D. and Denić-Jukić, V.: Groundwater balance estimation in karst by using a conceptual rainfallrunoff model, *J. Hydrol.*, 373, 302–315, <https://doi.org/10.1016/j.jhydrol.2009.04.035>, 2009.
- [Katz, B. G., Sepulveda, A. A., and Verdi, R. J.: Estimating Nitrogen Loading to Ground Water and Assessing Vulnerability to Nitrate Contamination in a Large Karstic Springs Basin, Florida1, \*JAWRA Journal of the American Water Resources Association\*, 45, 607–627, <https://doi.org/10.1111/j.1752-1688.2009.00309.x>, 2009.](https://doi.org/10.1111/j.1752-1688.2009.00309.x)
- 920 [Association](https://doi.org/10.1111/j.1752-1688.2009.00309.x), 45, 607–627, <https://doi.org/10.1111/j.1752-1688.2009.00309.x>, 2009.
- Kling, H., Fuchs, M., and Paulin, M.: Runoff conditions in the upper Danube basin under an ensemble of climate change scenarios, *J. Hydrol.*, 424–425, 264–277, <https://doi.org/10.1016/j.jhydrol.2012.01.011>, 2012.
- Knoben, W. J. M., Freer, J. E., and Woods, R. A.: Technical note: Inherent benchmark or not? Comparing Nash and Kling efficiency scores, *Hydrol. Earth Syst. Sci.*, 23, 4323–4331, <https://doi.org/10.5194/hess-23-4323-2019>, 2019.
- 925 Kogovšek, J., Knez, M., Mihevc, A., Petrič, M., Slabe, T., and Šebela, S.: Military training area in Kras (Slovenia), *Environ. Geol.*, 38, 69–76, <https://doi.org/10.1007/s002540050402>, 1999.
- Kong A Siou, L., Johannet, A., Borrell, V., and Pistre, S.: Complexity selection of a neural network model for karst flood forecasting: The case of the Lez Basin (southern France), *J. Hydrol.*, 403, 367–380, <https://doi.org/10.1016/j.jhydrol.2011.04.015>, 2011.
- 930 Kong A Siou, L., Fleury, P., Johannet, A., Borrell Estupina, V., Pistre, S., and Dörfliger, N.: Performance and complementarity of two systemic models (reservoir and neural networks) used to simulate spring discharge and piezometry for a karst aquifer, *J. Hydrol.*, 519, 3178–3192, <https://doi.org/10.1016/j.jhydrol.2014.10.041>, 2014.
- Kong A Siou, L., Johannet, A., Borrell Estupina, V., and Pistre, S.: Neural networks for karst groundwater management: Case of the Lez spring (Southern France), *Environ. Earth Sci.*, 74, 7617–7632, <https://doi.org/10.1007/s12665-015-4708-9>, 2015.
- 935 Kovačević, M., Ivanišević, N., Dašić, T., and Marković, L.: Application of artificial neural networks for hydrological modelling in Karst, *Graevinar*, 70, 2018.

- Kovačič, G.: Hydrogeological study of the Malenščica karst spring (SW Slovenia) by means of a time series analysis, *Acta Carsologica*, 39, <https://doi.org/10.3986/ac.v39i2.93>, 2010.
- 940 Kovács, A. and Sauter, M.: Modelling karst hydrodynamics, in: *Methods in Karst Hydrogeology*, edited by: Goldscheider, N. and Drew, D., Taylor & Francis, London, 201–222, 2007.
- Kurtulus, B. and Razack, M.: Evaluation of the ability of an artificial neural network model to simulate the input-output responses of a large karstic aquifer: The La Rochefoucauld aquifer (Charente, France), *Hydrogeol. J.*, 15, 241–254, <https://doi.org/10.1007/s10040-006-0077-5>, 2007.
- 945 Kurtulus, B. and Razack, M.: Modeling daily discharge responses of a large karstic aquifer using soft computing methods: Artificial neural network and neuro-fuzzy, *J. Hydrol.*, 381, 101–111, <https://doi.org/10.1016/j.jhydrol.2009.11.029>, 2010.
- LeCun, Y., Bengio, Y., and Hinton, G.: Deep learning, *Nature*, 521, 436–444, <https://doi.org/10.1038/nature14539>, 2015.
- Lehmann, P., Stauffer, F., Hinz, C., Dury, O., and Flühler, H.: Effect of hysteresis on water flow in a sand column with a fluctuating capillary fringe, *J. Contam. Hydrol.*, 33, 81–100, [https://doi.org/10.1016/S0169-7722\(98\)00066-7](https://doi.org/10.1016/S0169-7722(98)00066-7), 1998.
- 950 Lobligeois, F., Andréassian, V., Perrin, C., Tabary, P., and Loumagne, C.: When does higher spatial resolution rainfall information improve streamflow simulation? An evaluation using 3620 flood events, *Hydrol. Earth Syst. Sci.*, 18, 575–594, <https://doi.org/10.5194/hess-18-575-2014>, 2014.
- Makropoulos, C., Koutsoyiannis, D., Stanić, M., Djordjević, S., Prodanović, D., Dašić, T., Prohaska, S., Maksimović, Č., and Wheeler, H.: A multi-model approach to the simulation of large scale karst flows, *J. Hydrol.*, 348, 412–424, <https://doi.org/10.1016/j.jhydrol.2007.10.011>, 2008.
- 955 Martín-Algarra, A.: Evolucion geologica alpina del contacto entre las zonas internas y las zonas externas de la cordillera Bética (sector centro-occidental), PhD thesis, Universidad de Granada, 1987.
- Mauricio Zambrano-Bigiarini: hydroGOF: Goodness-of-fit functions for comparison of simulated and observed hydrological time series, Manual, <https://doi.org/10.5281/zenodo.839854>, 2020.
- 960 Mayaud, C., Gabrovšek, F., Blatnik, M., Kogovšek, B., Petrič, M., and Ravbar, N.: Understanding flooding in poljes: A modelling perspective, *J. Hydrol.*, 575, 874–889, <https://doi.org/10.1016/j.jhydrol.2019.04.092>, 2019.
- [Mayaud, C., Kogovšek, B., Gabrovšek, F., Blatnik, M., Petrič, M., and Ravbar, N.: Deciphering the water balance of poljes: example of Planinsko Polje \(Slovenia\), \*Acta Carsologica\*, 51, <https://doi.org/10.3986/ac.v51i2.11029>, 2022.](https://doi.org/10.3986/ac.v51i2.11029)
- Mazzilli, N. and Bertin, D.: KarstMod User Guide - version 2.2, hal-01832693, 103927, 2019.
- 965 Mazzilli, N., Guinot, V., and Jourde, H.: Sensitivity analysis of conceptual model calibration to initialisation bias. Application to karst spring discharge models, *Adv. Water Resour.*, 42, 1–16, <https://doi.org/10.1016/j.advwatres.2012.03.020>, 2012.
- Mazzilli, N., Guinot, V., Jourde, H., Lecoq, N., Labat, D., Arfib, B., Baudement, C., Danquigny, C., Soglio, L. D., and Bertin, D.: KarstMod: A modelling platform for rainfall - discharge analysis and modelling dedicated to karst systems, *Environ. Model. Softw.*, 122, 103927, <https://doi.org/10.1016/j.envsoft.2017.03.015>, 2019.
- 970

- McKinney, W.: Data Structures for Statistical Computing in Python, Proceedings of the 9th Python in Science Conference, 56–61, <https://doi.org/10.25080/Majora-92bf1922-00a>, 2010.
- [McMillan, H. K., Westerberg, I. K., and Krueger, T.: Hydrological data uncertainty and its implications, WIREs Water, 5, e1319, https://doi.org/10.1002/wat2.1319, 2018.](https://doi.org/10.1002/wat2.1319)
- 975 Meng, X., Yin, M., Ning, L., Liu, D., and Xue, X.: A threshold artificial neural network model for improving runoff prediction in a karst watershed, *Environ. Earth Sci.*, 74, 5039–5048, <https://doi.org/10.1007/s12665-015-4562-9>, 2015.
- Moges, E., Demissie, Y., Larsen, L., and Yassin, F.: Review: Sources of Hydrological Model Uncertainties and Advances in Their Analysis, *Water*, 13, 28, <https://doi.org/10.3390/w13010028>, 2021.
- Nash, J. E. and Sutcliffe, J.: River flow forecasting through conceptual models: Part 1. A discussion of principles., *J. Hydrol.*, 980 10, 282–290, 1970.
- Nogueira, F.: Bayesian Optimization: Open source constrained global optimization tool for Python, 2014.
- Ollivier, C., Mazzilli, N., Oliosio, A., Chalikakis, K., Carrière, S. D., Danquigny, C., and Emblanch, C.: Karst recharge-discharge semi distributed model to assess spatial variability of flows, *Sci. Total Environ.*, 703, 134368, <https://doi.org/10.1016/j.scitotenv.2019.134368>, 2020.
- 985 Onyutha, C.: Hydrological Model Supported by a Step-Wise Calibration against Sub-Flows and Validation of Extreme Flow Events, *Water*, 11, 244, <https://doi.org/10.3390/w11020244>, 2019.
- Oudin, L., Hervieu, F., Michel, C., Perrin, C., Andréassian, V., Anctil, F., and Loumagne, C.: Which potential evapotranspiration input for a lumped rainfallrunoff model?: Part 2 a simple and efficient potential evapotranspiration model for rainfallrunoff modelling, *J. Hydrol.*, 303, 290–306, <https://doi.org/10.1016/j.jhydrol.2004.08.026>, 2005.
- 990 Pedregosa, F., Varoquaux, G., Gramfort, A., Michel, V., Thirion, B., Grisel, O., Blondel, M., Müller, A., Nothman, J., Louppe, G., Prettenhofer, P., Weiss, R., Dubourg, V., Vanderplas, J., Passos, A., Cournapeau, D., Brucher, M., Perrot, M., and Duchesnay, É.: Scikit-learn: Machine Learning in Python, arXiv:1201.0490 [cs], 2018.
- Pelletier, P. M.: Uncertainties in the single determination of river discharge: A literature review, *Can. J. Civ. Eng.*, 15, 834–850, <https://doi.org/10.1139/l88-109>, 1988.
- 995 Pereira, D. dos R., Martinez, M. A., Almeida, A. Q. de, Pruski, F. F., Silva, D. D. da, and Zonta, J. H.: Hydrological simulation using SWAT model in headwater basin in Southeast Brazil, *Eng. Agric.*, 34, 789–799, <https://doi.org/10.1590/S0100-69162014000400018>, 2014.
- Perrin, J., Jeannin, P.-Y., and Zwahlen, F.: Epikarst storage in a karst aquifer: A conceptual model based on isotopic data, Milandre test site, Switzerland, *J. Hydrol.*, 279, 106–124, [https://doi.org/10.1016/S0022-1694\(03\)00171-9](https://doi.org/10.1016/S0022-1694(03)00171-9), 2003.
- 1000 Petric, M.: Chapter 10.3 - Case Study: Characterization, exploitation, and protection of the Malenščica karst spring, Slovenia, in: *Groundwater Hydrology of Springs*, edited by: Kresic, N. and Stevanovic, Z., Butterworth-Heinemann, Boston, 428–441, <https://doi.org/10.1016/B978-1-85617-502-9.00021-9>, 2010.
- R Core Team: R: A language and environment for statistical computing. R Foundation for Statistical Computing, Vienna, Austria. URL <https://www.R-project.org/>, 2021. Last access: 12 October 2022.

- 1005 Ravbar, N., Barberá, J. A., Petrič, M., Kogovšek, J., and Andreo, B.: The study of hydrodynamic behaviour of a complex karst system under low-flow conditions using natural and artificial tracers (the catchment of the Unica River, SW Slovenia), *Environ. Earth Sci.*, 65, 2259–2272, <https://doi.org/10.1007/s12665-012-1523-4>, 2012.
- Reback, J., jbrockmendel, McKinney, W., Bossche, J. V. den, Augspurger, T., Cloud, P., Hawkins, S., Roeschke, M., gfyong, Sinhrks, Klein, A., Petersen, T., Hoefler, P., Tratner, J., She, C., Ayd, W., Naveh, S., Garcia, M., Darbyshire, J. H.
- 1010 M., Schendel, J., Hayden, A., Shadrach, R., Saxton, D., Gorelli, M. E., Li, F., Zeitlin, M., Jancauskas, V., McMaster, A., Battiston, P., and Seabold, S.: Pandas-dev/pandas: Pandas 1.3.5, <https://doi.org/10.5281/zenodo.5774815>, 2021.
- Refsgaard, J. C., van der Sluijs, J. P., Højberg, A. L., and Vanrolleghem, P. A.: Uncertainty in the environmental modelling process A framework and guidance, *Environ. Model. Softw.*, 22, 1543–1556, <https://doi.org/10.1016/j.envsoft.2007.02.004>, 2007.
- 1015 Santos, L., Thirel, G., and Perrin, C.: Technical note: Pitfalls in using log-transformed flows within the KGE criterion, *Hydrol. Earth Syst. Sci.*, 22, 4583–4591, <https://doi.org/10.5194/hess-22-4583-2018>, 2018.
- Schwemmler, R., Demand, D., and Weiler, M.: Technical note: Diagnostic efficiency specific evaluation of model performance, *Hydrol. Earth Syst. Sci.*, 25, 2187–2198, <https://doi.org/10.5194/hess-25-2187-2021>, 2021.
- Seibert, J.: Reliability of Model Predictions Outside Calibration Conditions: Paper presented at the Nordic Hydrological Conference (Røros, Norway 4-7 August 2002), *Hydrol. Res.*, 34, 477–492, <https://doi.org/10.2166/nh.2003.0019>, 2003.
- 1020 Sezen, C., Bezak, N., Bai, Y., and Šraj, M.: Hydrological modelling of karst catchment using lumped conceptual and data mining models, *J. Hydrol.*, 576, 98–110, <https://doi.org/10.1016/j.jhydrol.2019.06.036>, 2019.
- Sidle, R. C.: Field observations and process understanding in hydrology: Essential components in scaling, *Hydrol. Process.*, 20, 1439–1445, <https://doi.org/10.1002/hyp.6191>, 2006.
- 1025 Sidle, R. C.: Strategies for smarter catchment hydrology models: Incorporating scaling and better process representation, *Geosci. Lett.*, 8, 24, <https://doi.org/10.1186/s40562-021-00193-9>, 2021.
- Singh, S. K. and Bárdossy, A.: Calibration of hydrological models on hydrologically unusual events, *Adv. Water Resour.*, 38, 81–91, <https://doi.org/10.1016/j.advwatres.2011.12.006>, 2012.
- SNO KARST: Time series of type hydrology-hydrogeology in Le Lez (Méditerranée) basin - MEDYCYSS observatory -
- 1030 KARST observatory network - OZCAR Critical Zone network Research Infrastructure, <https://doi.org/10.15148/CFD01A5B-B7FD-41AA-8884-84DBDDAC767E>, 2019.
- Srivastava, N., Hinton, G., Krizhevsky, A., Sutskever, I., and Salakhutdinov, R.: Dropout: A Simple Way to Prevent Neural Networks from Overfitting, *J. Mach. Learn. Res.*, 15, 1929–1958, 2014.
- Stevanović, Z.: Karst waters in potable water supply: A global scale overview, *Environ. Earth Sci.*, 78, 662, <https://doi.org/10.1007/s12665-019-8670-9>, 2019.
- 1035 Thoen, E.: Padr: Quickly get datetime data ready for analysis. <https://CRAN.R-project.org/package=padr>, Manual, 2021. Last access: 12 October 2022.

- Tritz, S., Guinot, V., and Jourde, H.: Modelling the behaviour of a karst system catchment using non-linear hysteretic conceptual model, *J. Hydrol.*, 397, 250–262, <https://doi.org/10.1016/j.jhydrol.2010.12.001>, 2011.
- 1040 van der Walt, S., Colbert, S. C., and Varoquaux, G.: The NumPy Array: A Structure for Efficient Numerical Computation, *Comput. Sci. Eng.*, 13, 22–30, <https://doi.org/10.1109/MCSE.2011.37>, 2011.
- van Rossum, G.: Python Tutorial, 1995.
- Van, S. P., Le, H. M., Thanh, D. V., Dang, T. D., Loc, H. H., and Anh, D. T.: Deep learning convolutional neural network in rainfallrunoff modelling, *J. Hydroinformatics*, 22, 541–561, <https://doi.org/10.2166/hydro.2020.095>, 2020.
- 1045 Wendling, U. and Müller, J.: Entwicklung eines Verfahrens zur rechnerischen Abschätzung der Verdunstung im Winter., *Z. Meteorol.*, 34, 82–85, 1984.
- [Westerberg, I. K., Wagener, T., Coxon, G., McMillan, H. K., Castellarin, A., Montanari, A., and Freer, J.: Uncertainty in hydrological signatures for gauged and ungauged catchments, \*Water Resources Research\*, 52, 1847–1865, <https://doi.org/10.1002/2015WR017635>, 2016.](https://doi.org/10.1002/2015WR017635)
- 1050 Wickham, H., Averick, M., Bryan, J., Chang, W., McGowan, L. D., François, R., Grolemund, G., Hayes, A., Henry, L., Hester, J., Kuhn, M., Pedersen, T. L., Miller, E., Bache, S. M., Müller, K., Ooms, J., Robinson, D., Seidel, D. P., Spinu, V., Takahashi, K., Vaughan, D., Wilke, C., Woo, K., and Yutani, H.: Welcome to the tidyverse, *J. Open Source Softw.*, 4, 1686, <https://doi.org/10.21105/joss.01686>, 2019.
- Wilke, C. O.: Cowplot: Streamlined plot theme and plot annotations for 'Ggplot2', Manual, 2020.
- 1055 [Wilks, D. S.: Statistical Forecasting, in: \*International Geophysics\*, vol. 100, Elsevier, 215–300, <https://doi.org/10.1016/B978-0-12-385022-5.00007-5>, 2011.](https://doi.org/10.1016/B978-0-12-385022-5.00007-5)
- [Willmott, C. J., Robeson, S. M., and Matsuura, K.: A refined index of model performance, \*Intern. J. Climatol.\*, 32, 2088–2094, <https://doi.org/10.1002/joc.2419>, 2012.](https://doi.org/10.1002/joc.2419)
- Wu, Q., Xu, H., and Pang, W.: GIS and ANN coupling model: An innovative approach to evaluate vulnerability of karst water inrush in coalmines of north China, *Environ. Geol.*, 54, 937–943, <https://doi.org/10.1007/s00254-007-0887-3>, 2008.
- Wunsch, A., Liesch, T., and Broda, S.: Groundwater level forecasting with artificial neural networks: A comparison of long short-term memory (LSTM), convolutional neural networks (CNNs), and non-linear autoregressive networks with exogenous input (NARX), *Hydrol. Earth Syst. Sci.*, 25, 1671–1687, <https://doi.org/10.5194/hess-25-1671-2021>, 2021.
- Wunsch, A., Liesch, T., Cinkus, G., Ravbar, N., Chen, Z., Mazzilli, N., Jourde, H., and Goldscheider, N.: Karst spring discharge modeling based on deep learning using spatially distributed input data, *Hydrol. Earth Syst. Sci.*, 26, 2405–2430, <https://doi.org/10.5194/hess-26-2405-2022>, 2022.
- 1065 Xie, Y., Allaire, J. J., and Grolemund, G.: R markdown: The definitive guide, Chapman and Hall/CRC, Boca Raton, Florida, 2018.
- Xie, Y., Dervieux, C., and Riederer, E.: R markdown cookbook, Chapman and Hall/CRC, Boca Raton, Florida, 2020.
- 1070 Yin, D., Shu, L., Chen, X., Wang, Z., and Mohammed, M. E.: Assessment of Sustainable Yield of Karst Water in Huaibei, China, *Water Resour. Manage.*, 25, 287–300, <https://doi.org/10.1007/s11269-010-9699-4>, 2011.

Zhang, J. L., Li, Y. P., Huang, G. H., Wang, C. X., and Cheng, G. H.: Evaluation of Uncertainties in Input Data and Parameters of a Hydrological Model Using a Bayesian Framework: A Case Study of a Snowmelt–Precipitation-Driven Watershed, Journal of Hydrometeorology, 17, 2333–2350, <https://doi.org/10.1175/JHM-D-15-0236.1>, 2016.

1075 Zhou, B.-Q., Yang, Z., Hu, R., Zhao, X.-J., and Chen, Y.-F.: Assessing the impact of tunnelling on karst groundwater balance by using lumped parameter models, J. Hydrol., 599, 126375, <https://doi.org/10.1016/j.jhydrol.2021.126375>, 2021.